Published in : The Plant Cell (2024), vol. 36, n°10, pp. 4491–4510
DOI: 10.1093/plcell/koae209
Status : Postprint (Author's version)

THE TRANSCRIPTION FACTORS ZAT5 AND BLH2/4 REGULATE HOMOGALACTURONAN DEMETHYLESTERIFICATION IN ARABIDOPSIS SEED COAT MUCILAGE

Minmin Xie,[1,2,3,†] Anming Ding,[1,†] Yongfeng Guo,[1] Jinhao Sun,[1,4] Wanya Qiu,[1,5] Mingli Chen,[1] Zhiyuan Li,[1]

Shanshan Li,[1,5] Gongke Zhou,[6] Yan Xu,[7] Meng Wang,[1,6] Aurore Richel,[3,*] Daping Gong,[1,*] Yingzhen Kong[1,6,*]

1Key Laboratory of Tobacco Gene Resources, Biotechnology Center, Tobacco Research Institute, Chinese Academy of Agricultural Sciences (CAAS), Qingdao 266101, China
2Graduate School of Chinese Academy of Agricultural Science, Beijing 100081, China
3Laboratory of Biomass and Green Technologies, Gembloux Agro-Bio Tech, University of Liege, Gembloux 5030, Belgium
4Technology Center, China Tobacco Jiangsu Industrial Co., Ltd., Nanjing 210019, China
5Key Laboratory of Natural Products Synthetic Biology of Ethnic Medicinal Endophytes, State Ethnic Affairs Commission, Yunnan Minzu University, Kunming 650031, China
6College of Agronomy, Qingdao Agricultural University, Qingdao 266109, China
7Key Laboratory of Biofuels, Qingdao Engineering Research Center of Biomass Resources and Environment, Qingdao Institute of Bioenergy and Bioprocess Technology, Chinese Academy of Sciences, Qingdao 266101, China

*Author for correspondence: kongyzh@qau.edu.cn (Y.K.), gongdaping@caas.cn (D.G.), a.richel@uliege.be (A.R.)

† These authors contributed equally.

The authors responsible for distribution of materials integral to the findings presented in this article in accordance with the policy described in the Instructions for Authors (https://academic.oup.com/plcell/pages/General-Instructions) are: Minmin Xie (xieminmin@caas.cn); Yingzhen Kong (kongyzh@qau.edu.cn).

ABSTRACT

The level of methylesterification alters the functional properties of pectin, which is believed to influence plant growth and development. However, the mechanisms that regulate demethylesterification remain largely unexplored. Pectin with a high degree of methylesterification is produced in the Golgi apparatus and then transferred to the primary cell wall where it is partially demethylesterified by pectin methylesterases (PMEs). Here, we show that in Arabidopsis (*Arabidopsis thaliana*) seed mucilage, pectin demethylesterification is negatively regulated by the transcription factor ZINC FINGER FAMILY PROTEIN5 (ZAT5). Plants carrying null mutations in *ZAT5* had increased PME activity, decreased pectin methylesterification, and produced seeds with a thinner mucilage layer. We provide evidence that ZAT5 binds to a TGATCA motif and thereby negatively regulates methylesterification by reducing the expression of *PME5*, *HIGHLY METHYL ESTERIFIED SEEDS* (*HMS*)/*PME6*, *PME12*, and *PME16*. We also demonstrate that ZAT5 physically interacts with BEL1-LIKE

Published in : The Plant Cell (2024), vol. 36, n°10, pp. 4491–4510
DOI: 10.1093/plcell/koae209
Status : Postprint (Author's version)

HOMEODOMAIN2 (BLH2) and BLH4 transcription factors. BLH2 and BLH4 are known to modulate pectin demethylesterification by directly regulating *PME58* expression. The ZAT5-BLH2/4 interaction provides a mechanism to control the degree of pectin methylesterification in seed coat mucilage by modifying each transcription factor's ability to regulate the expression of target genes encoding PMEs. Taken together, these findings reveal a transcriptional regulatory module comprising ZAT5, BLH2, and BLH4, that functions in modulating the demethylesterification of homogalacturonan in seed coat mucilage.

Introduction

The primary walls of growing plant cells are dynamic structures that are composed of cellulose, hemicellulose, and pectin together with small amounts of protein (Moller et al. 2012; Peaucelle et al. 2012). Pectin accounts for up to 35% of the primary cell wall in dicots and nongraminaceous monocots (Caffall and Mohnen 2009). It is a structurally complex polysaccharide comprising 4 domains: homo- galacturonan (HG), xylogalacturonan (XGA), rhamnogalacturonan-I (RG-I), and RG-II. HG is a linear homopolymer of 1,4-linked α -D-GalA. In XGA, β-D-xylose is attached to *O-3* of the HG backbone. The RG-I backbone comprises the disaccharide repeating unit [α-D-GalA-1,2-α-L-Rha-1,4]. RG-II has an HG backbone with up to 6 structurally distinct side chains attached to it (Zablackis et al. 1995; Caffall and Mohnen 2009; Mohnen et al. 2012; Duan et al. 2020). Pectin synthesis is believed to require at least 67 distinct transferase activities (Atmodjo et al. 2013).

HG, which accounts for about 65% of primary cell wall pectin, is produced as a highly methylesterified form (~80%) in the Golgi apparatus and then secreted into the cell wall (Wolf et al. 2009). This HG may then be modified by pectin methylesterases (PMEs). PME activity is often modulated by pectin methylesterase inhibitor proteins (PMEIs) (Wolf et al. 2009; Senechal et al. 2014). The Arabidopsis (*Arabidopsis thaliana*) genome encodes 66 putative PMEs and 71 potential PMEIs (Wang et al. 2013). Demethylesterified HG is a substrate for pectate lyases and polygalacturonases, which may allow cell wall physical properties to be altered. Demethylesterified HG interacts with Ca^{2+} to form cross-linked structures that contribute to cell wall strengthening (Wormit and Usadel 2018). Additionally, specific patterns of HG dimethylesterification may serve as anchoring platforms for cell wall proteins including Class III peroxidases (CIII PRXs) (Francoz et al. 2019; Dauphin et al. 2022). The methanol and oli- gogalacturonides produced during demethylesterification may act as signaling molecules in response to internal or external stimuli (Ridley et al. 2001; Wormit and Usadel 2018). The degree and pattern of pectin methylesterification are now understood to influence cell wall properties and contribute to developmental and stress responses in plants. Nevertheless, the precise molecular mechanisms governing pectin demethylesterification remain insufficiently studied.

Many angiosperms, including *Arabidopsis*, produce mature dry seeds that release a gelatinous mucilage capsule on the seed coat epidermis when exposed to water. *Arabidopsis* seed mucilage is rich in unbranched RG-I and also contains small amounts of HG, cellulose, and hemicellulose (Macquet et al. 2007; Harpaz-Saad et al. 2012; Yu et al. 2014). Mucilage is produced in large amounts from 5 to 8 d postanthesis (DPA) and secreted to

Published in : The Plant Cell (2024), vol. 36, n°10, pp. 4491–4510
DOI: 10.1093/plcell/koae209
Status : Postprint (Author's version)

the junction of outer tangential and radial cell walls. This generates a cytoplasmic column encircled by a donut-shaped pocket of mucilage. A volcano-shaped secondary wall, which displaces the cytoplasmic column, is produced after mucilage deposition (9 to 11 DPA). The mucilage released from mature hydrated seeds exists as 2 layers, a nonadherent mucilage (NM) layer that is solubilized with water and an adherent mucilage (AM) layer that requires ultrasonication to detach it from the seed (Zhao et al. 2017; Sola et al. 2019). The seed coat mucilage of *Arabidopsis* is now recognized as a model system to study the synthesis, modification, and interaction of polysaccharides, especially pectin (Sola et al. 2019). More than 80 genes, including those that encode functional proteins and transcription factors, have been identified and shown to be required for seed mucilage production, modification, and release (Xu et al. 2023).

The importance of HG demethylesterification in maintaining seed coat mucilage release and structure has been demonstrated by showing that several PMEs and PMEIs are required for the process to occur normally. For example, PME activity during mucilage modification is believed to be regulated by the subtilisin-like protease (SBT) SBT1.7. The seeds of *sbt1.7* mutants have altered degree of methylesterification (DM) of HG, do not release mucilage, and float on water (Rautengarten et al. 2008). Seed mucilage release in the *pmei6* mutants is retarded. PMEI6 inhibits endogenous PME activities. The mucilage phenotype of *pmei6 sbt1.7* double mutants exhibits additive properties, suggesting that SBT1.7 and PMEI6 regulate different PME enzymes (Saez-Aguayo et al. 2013). *HIGHLY METHYL ESTERIFIED SEEDS* (*HMS*)/*PME6* is highly expressed in the seed coat and the embryo during seed development. The enzyme is believed to regulate the DM of HG in the embryo and thereby facilitate wall loosening and cell expansion. Mutating *HMS*/*PME6* also indirectly influences seed mucilage extrusion (Levesque-Tremblay et al. 2015a). *PME58* was the first gene encoding a PME functioning primarily in the seed coat to be identified (Turbant et al. 2016). PME58 directly regulates pectin DM in seed mucilage. PMEI13 and PMEI14 have been reported to regulate HG DM in seed mucilage by inhibiting PME activity (Shi et al. 2018; Ding et al. 2021).

The seed coat mucilage system has been used to show that several transcription factors (TFs) modulate pectin demethylesterification. These include LEUNIG_HOMOLOG (LUH)/MUM1 (Huang et al. 2011), SEEDSTICK (STK) (Ezquer et al. 2016), MYB52 (Shi et al. 2018), ERF4 (Ding et al. 2021), and BEL1-LIKE HOMEODOMAIN2 (BLH2)/BLH 4 (Xu et al. 2020). They act by targeting downstream genes and have a positive or negative role in pectin demethylesterification. For example, LUH/MUM1 positively regulates *SBT1.7* and *PMEI6* (Huang et al. 2011), whereas STK positively regulates *PMEI6* (Ezquer et al. 2016). MYB52 directly activates the expression of *PMEI6*, *PMEI14*, and *SBT1.7* (Shi et al. 2018). ERF4 negatively regulates the expression of *PMEI13*/*14*/*15* and *SBT1.7*. ERF4 and MYB52 work in opposition to regulate the

HG DM of seed coat mucilage (Ding et al. 2021). By contrast, BLH2 and BLH4 were reported to regulate HG demethylesterifica- tion by directly activating *PME58* (Xu et al. 2020).

In this study, we show that a C2H2-type zinc-finger transcription factor (ZAT5) has a role in pectin demethylesterification of *Arabidopsis* seed mucilage. ZAT5 controls pectin DM by negatively regulating *PME5*, *HMS*/*PME6*, *PME12*, and *PME16* directly. The TGATCA motif in the promoters of the 4 *PMEs* is the recognition sequence for ZAT5. Our data also provide evidence that ZAT5 and BLH2/4 have antagonistic roles in regulating pectin DM by targeting PMEs.

Published in : The Plant Cell (2024), vol. 36, n°10, pp. 4491–4510
DOI: 10.1093/plcell/koae209
Status : Postprint (Author's version)

Results

EXPRESSION PROFILING OF ZAT5 IN DEVELOPING SEEDS

We found a group of genes that are differently expressed during the formation of seed mucilage using published microarray datasets of laser-capture microdissected *Arabidopsis* seed samples throughout distinct developmental phases (GSE12404) (Affymetrix ATH1 array—http://seedgenenetwork.net/arabidopsis) (Belmonte et al. 2013). Of these, *ZAT5* was significantly upregulated, implying a potential function of ZAT5 in the development of the seed coat. Public transcriptome data show that *ZAT5* is expressed in the chalazal seed coat (CZSC) and the general seed coat, with additional expression in the peripheral endosperm (http://seedgenenetwork.net/ arabidopsis; Supplementary Fig. S1). We used quantitative realtime PCR (qPCR) to investigate the expression of *ZAT5* in developing seeds at 4 DPA and in seed coats after 7, 10, and 13 DPA (Fig. 1A). *ZAT5* transcripts were detected at all 4 time points. Expressions reached a maximum level between 7 and 10 DPA and then decreased at 13 DPA.

To examine tissue-specific expression of *ZAT5*, expression of a β-glucuronidase (GUS) gene controlled by the 2,014 bp region upstream of ATG in *ZAT5* was determined. The GUS signal was detected in many tissues, including seedling, leaf and reproductive tissues (Fig. 1; Supplementary Fig. S2). Strong GUS staining was also detected in the coat epidermal cells of developing seeds, as well as in the mucilage released from the seed coat epidermal cells at the 10 to 13 DPA stages (Fig. 1, B to E). We next located the GUS signal in sections of developing seeds at 10 and 13 DPA. There was a clear signal in the CZSC, seed coat epidermal cells, embryo and peripheral endosperm at both stages (Fig. 1, F and G). Our GUS histochemical assays are consistent with ZAT5 having a role in the metabolism of seed mucilage.

We next performed an in situ hybridization assay to more precisely localize the expression of *ZAT5*. *ZAT5* was strongly expressed in seed coat epidermal cells at 7 to 10 DPA and much more at 13 DPA. *ZAT5* transcripts were also detected in the embryo and peripheral endosperm at 10 to 13 DPA (Fig. 1H), indicating that *ZAT5* is expressed extensively in the developing seeds. Our expression analyzes data prompted us further to characterize the role of ZAT5 in seed coat mucilage formation.

ZAT5 IS A TYPICAL C2H2-TYPE ZINC-FINGER PROTEIN

ZAT5 contains an 861 bp ORF that encodes 286 amino acids. The calculated molecular mass of ZAT5 (GenBank accession AEC08090) is 31.367 kDa (Supplementary Fig. S3A). ZAT5 belongs to the C1-2i subclass of the C2H2-type zinc-finger protein (ZFP) family, which is one of the biggest TF families in plants. Our phylogenetic tree shows that the C1-2i subclass contains 20 members (Supplementary Fig. S3B).

Published in : The Plant Cell (2024), vol. 36, n°10, pp. 4491–4510
DOI: 10.1093/plcell/koae209
Status : Postprint (Author's version)

***Figure 1**. Expression profiling of ZAT5 in developing seeds*

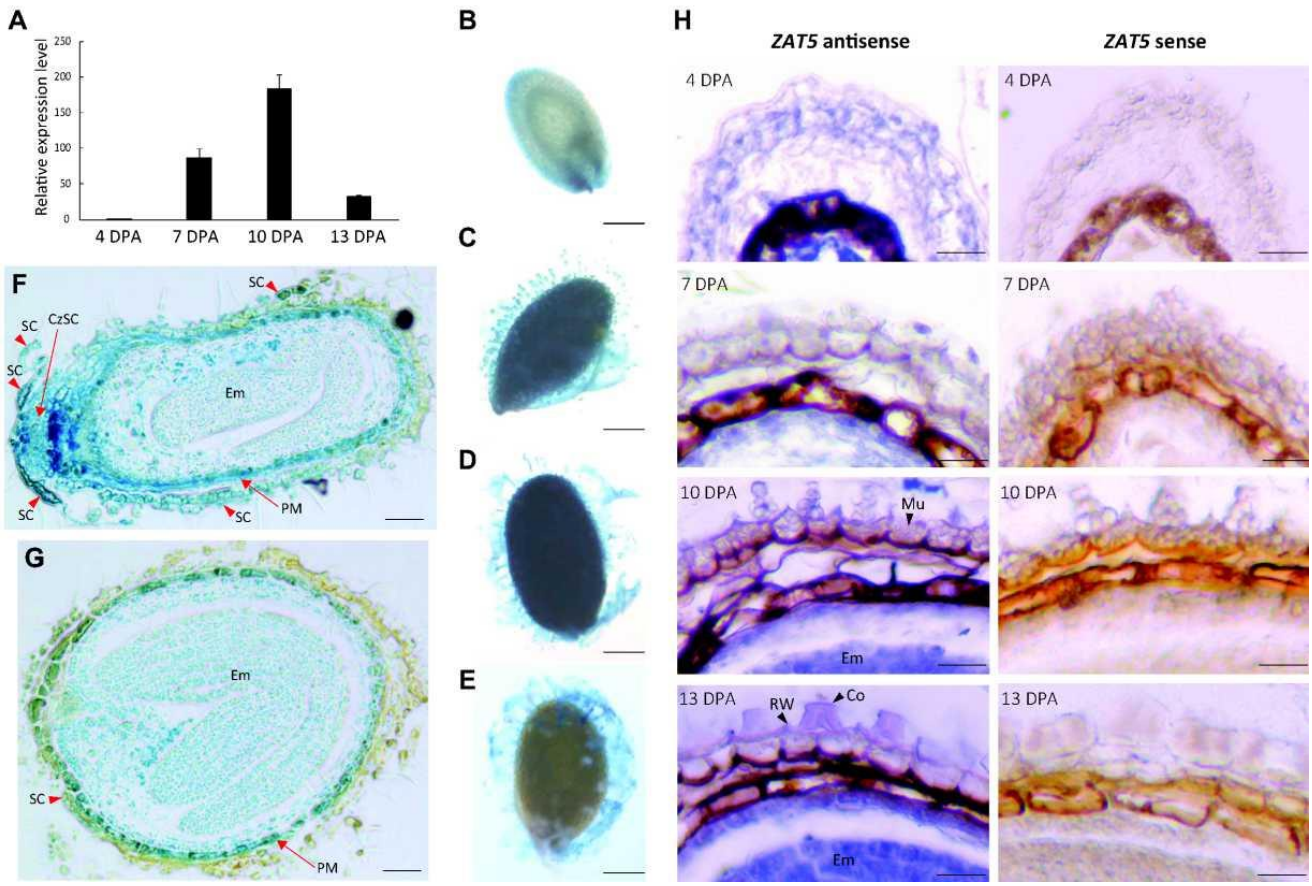

A) qPCR analysis of *ZAT5* in 4 DPA seeds and 7, 10, and 13 DPA seed coats. Gene expression is shown relative to *ACTIN2*. The gene expression level at 4 DPA was set to 1. SD is shown with error bars (n = 3). B to G) Histochemical analysis of GUS activity in *ProZAT5:GUS* transgenic *Arabidopsis* tissues. B) Four DPA seed; C) 7 DPA seed; D) 10 DPA seed; E) 13 DPA seed. GUS staining seed sections at 10 (F) and 13 (G) DPA. Bars = (B to E) 1,000 and (F, G) 50 µm. H) In situ hybridization of *ZAT5* transcripts in the seed coat of 4, 7, 10, and 13 DPA. Bars = 20 µm. SC, seed coat; CZSC, Chalazal seed coat; Em, embryo; PM, peripheral endosperm; Mu, mucilage; Co, columella; and RW, radial cell wall.

Most of the C1-2i members, including ZAT5, have highly conserved QALGGH motifs responsible for DNA binding and a predicted nuclear localization signal named B-box (KXKRSKRXR) at their N-terminus. A DLNL core sequence (DLN-box) named the ethylene-responsive element binding-factor-associated amphiphilic repression (EAR) domain is at the C-terminus (Supplementary Fig. S3A). Many C2H2 ZFPs including ARABIDOPSIS ZINC-FINGER PROTEIN 1 (AZF1), AZF2, AZF3, ZAT7, ZAT10, and ZAT12 that have an EAR domain are transcriptional repressors (Xie et al. 2019).

Subcellular localization of proteins may help to determine their potential roles. Transcription factors work primarily by binding to gene promoters in the nucleus. We examined the subcellular location of ZAT5, by transforming *Nicotiana benthamiana* leaves with a *Pro35S:ZAT5-GFP* construct. The results of transient expression showed that the ZAT5-GFP fusion signal was predominantly observed in the nucleus (Supplementary Fig. S4), indicating that ZAT5 is a nuclear protein.

Published in : The Plant Cell (2024), vol. 36, n°10, pp. 4491–4510
DOI: 10.1093/plcell/koae209
Status : Postprint (Author's version)

THE ZAT5 MUTANTS EXHIBIT A DEFECTIVE MUCILAGE PHENOTYPE

To determine if ZAT5 affects seed coat mucilage formation, 2 independent homozygous mutant alleles (SAIL_13_H11 and SALK_048250) were obtained from the Arabidopsis Biological Resource Center (ABRC). Both contain a T-DNA insertion in the *ZAT5* coding region (Fig. 2A). These 2 homozygous lines were named *zat5-1* and *zat5-2*, respectively. No amplification was obtained in *zat5-1* or *zat5-2* by RT-PCR using primers placed on the 5'-side or 3'-side of their T-DNA insertion. No full-length

transcript was produced from both *zat5* mutants when primers covering the complete *ZAT5* coding sequence (CDS) were used (Fig. 2B). Thus, *zat5-1* and *zat5-2* are both null mutants.

The seed mucilage phenotypes of *zat5-1* and *zat5-2* mutants were examined using ruthenium red (RR) staining. The 2 mutants and wild type (WT) had no discernible differences when the seeds were stained without shaking in water. However, after shaking the seeds in water for 2 h at 200 rpm the stained halo of the *zat5-1* and *zat5-2* mucilage was thinner and the volume of their mucilage layer was significantly reduced compared to that of the WT (Fig. 2, C and D). This defect was complemented by transforming *zat5* with the *ProZAT5:ZAT5* construct, suggesting that the mucilage defect is likely caused by mutating *ZAT5*. Additionally, we crossed the *zat5* mutants (female parent) and WT (male parent) to generate F1 seeds. The mucilage phenotype of the F1 seeds and the *zat5* mutants were similar (Fig. 2, C and D). Moreover, there were no significant differences in the relative volume of de-mucilaged seeds (Supplementary Fig. S5). Thus, the function of ZAT5 in the seed coat is likely to account for the visible phenotypes because the seed coat in F1 seeds is homozygous for *zat5* but the embryo is heterozygous for the mutation.

To investigate whether the *zat5* mucilage defect is caused by abnormal seed coat differentiation, we used scanning electron microscopy (SEM) to observe the seed coat surface. No discernible differences were observed in the morphology of *zat5* or WT seed coats (Supplementary Fig. S6).

Published in : The Plant Cell (2024), vol. 36, n°10, pp. 4491–4510
DOI: 10.1093/plcell/koae209
Status : Postprint (Author's version)

***Figure 2**. Zat5 mutants have a defective AM phenotype*

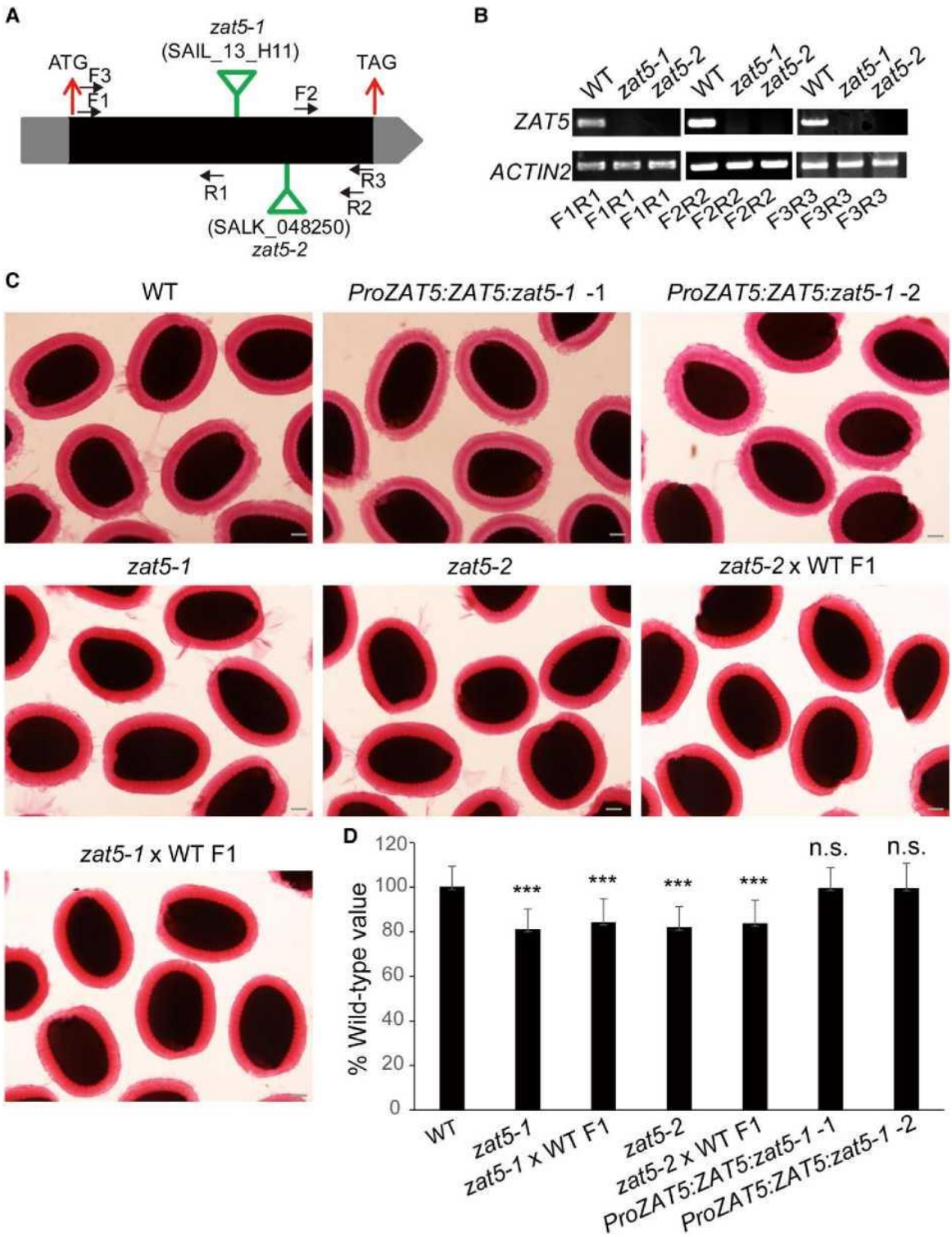

A) The T-DNA insert sites of SAIL_13_H11 (*zat5-1*) and SALK_048250 (*zat5-2*). The black and gray boxes represent the exon and untranslated regions, respectively. The T-DNA insert sites of *zat5-1* and *zat5-2* are indicated by the inverted triangles. The arrows indicate the primers used in RT-PCR. B) RT-PCR shows the absence of *ZAT5* transcript in the *zat5* mutants. C) The mucilage phenotypes of WT, *zat5*, F1 progeny of the cross between *zat5* (female parent) and WT (male parent), and *ProZAT5:ZAT5:zat5-1* seeds after shaking for 2 h in water at 200 rpm and staining with RR. Scale bar = 100 µm. D) The relative volume of AM layers. The WT seed average volume

Published in : The Plant Cell (2024), vol. 36, n°10, pp. 4491–4510
DOI: 10.1093/plcell/koae209
Status : Postprint (Author's version)

was set to 100%. SD is shown with error bars (*n*= 150 for WT and mutant seeds; *n*= 60 for F1 hybrid seeds). Asterisks indicate significant differences compared with the WT (n.s., not significant; ***$P < 0.001$) determined using the one-way ANOVA followed by Dunnett's multiple comparison test.

MONOSACCHARIDE COMPOSITION HAS NO CHANGE IN ZAT5 SEED MUCILAGE

Since treating seeds with water allows mucilage release to be visualized, treatment with the divalent cationic chelator EDTA is thought to affect the ionic cross-linking between the HG chains and thus alter the adhesion ability of the adherent layer (Ezquer et al. 2016; Turbant et al. 2016), mucilage was released from mature, dry seeds by treatment with water or with EDTA to quantify the amounts of material in the adherent and nonadherent layers. We then determined the monosaccharide composition of the NM and AM using high performance liquid chromatography (HPLC). The *zat5* mutants and WT seed mucilage had similar monosaccharide compositions, and there were no significant differences in the total sugars present in the material solubilized with water or EDTA (Table 1; Supplementary Fig. S7). These results show that ZAT5 has no discernible effect on the amounts and composition of seed mucilage polysaccharide produced.

PECTIN METHYLESTERIFICATION AND PME ACTIVITY ARE ALTERED IN ZAT5 MUCILAGE

To determine if the pectin DM level differs in *zat5* seed mucilage, we measured the amounts of methanol produced when whole mucilage was treated with alkali (Voiniciuc et al. 2013). Significantly lower amounts of methanol were released from *zat5-1* and *zat5-2* seeds than from WT seeds (Fig. 3A).

We next immunolabeled mature seeds with monoclonal antibodies (mAbs) to obtain data on the pattern of HG methylesterification and further demonstrate that ZAT5 affects the pectin DM of seed mucilage. JIM5 recognizes lowly methylesterified HG, JIM7 recognizes partially methylesterified HG, and CCRC38 labels HG lacking methyl esters (Röckel et al. 2008). The signal for JIM7 was mainly distributed at the outer periphery of the adherent layer in WT as previously reported (Wang et al. 2019; Xu et al. 2020). *zat5* mucilage exhibited much lower JIM7 labeling intensity than WT (Fig. 3C). Signals for CCRC-M38 and JIM5 were mainly detected in the columella and alongside the ray structure in the inner regions of the AM in WT. The labeling intensity of *zat5* by JIM5 was lower than that of the WT, especially in the regions between ray structures (Fig. 3D). By contrast, the CCRC-M38 labeling intensity of *zat5* mucilage was a little stronger than that of the WT (Fig. 3E). We also used the same mAbs to quantify the status of HG in AM using enzyme linked immunosorbent assays (ELISA). Stronger binding of CCRC-M38 and weaker binding of JIM5 and JIM7 were observed with *zat5-2* mucilage compared to WT mucilage (Supplementary Fig. S8). These results suggest that in *zat5* mucilage there is a reduction in highly and moderately methylesterified HGs and an increase in un-methylesterified HG. Since HG DM is altered by PMEs, we next examined if the decreased level of HG DM in *zat5* mutants is associated with PME activity. As shown in Fig. 3B, PME activity in the 7 to 10 DPA seed coat of both *zat5* mutants was increased compared with that in the WT. These results are consistent with a decrease in DM of *zat5* seed mucilage. Thus, ZAT5 may regulate the DM of seed mucilage pectin by suppressing PME activity.

Published in : The Plant Cell (2024), vol. 36, n°10, pp. 4491–4510
DOI: 10.1093/plcell/koae209
Status : Postprint (Author's version)

ZAT5 DOWNREGULATES PME5, HMS/PME6, PME12, AND PME16

We next used whole transcriptome RNA-sequencing (RNA-seq) of 7 to 8 DPA developing seeds dissected from WT and *zat5* siliques to identify how ZAT5 affects the DM of seed mucilage pectin. Potentially, 30 genes were upregulated and 173 genes were down- regulated in *zat5*. Several of these differentially expressed genes (DEGs) were associated with cell wall polysaccharides, including several *PME* genes such as *PME4*, *PME5*, *HMS/PME6*, *PME12*, *PME16*, *PME48*, *PME58*, and *PME65* (Supplementary Data Set 1). Data from the *Arabidopsis* eFP browser database (http://bar. utoronto.ca/efp/cgi-bin/efpWeb.cgi; Supplementary Fig. S9) indicates that the expression of *PME4*, *48*, and *65* is low in the seed coat at all developmental stages. In contrast, *PME5*, *6*, *12*, *16*, and *58* are differentially expressed in the seed coat at different developmental stages (Le et al. 2010). To quantify the gene expression level more accurately, we further determined the expression level of *PME5*, *6*, *12*, *16*, and *58* by qPCR using the dissected seed coats. These 5 genes were all significantly upregulated and down-regulated in *zat5* and seeds overexpressing *ZAT5*, respectively, compared to in WT (Fig. 4A). This is in accordance with our data that in *zat5* mutants the decrease in pectin DM results from increased PME activity (Fig. 3). These findings suggest that ZAT5 could negatively regulate the expression of *PME5*, *HMS/PME6*, *PME12*, *PME16*, and *PME58*.

A dual-luciferase (LUC) activity assay was then used to determine if *PME5*, *HMS/PME6*, *PME12*, *PME16*, and *PME58* are direct targets of ZAT5. Co-transfection of pGreenII 62-sk-ZAT5 (overexpression) and pGreenII 0800-LUC with the promoters of *PME5*, *HMS/PME6*, *PME12*, and *PME16* significantly impeded LUC activity compared to controls (Fig. 4, B and C). LUC activity was reduced at least 2.5-fold when ZAT5 was introduced (Fig. 4C), suggesting that ZAT5 has strong inhibitory activity. By contrast, altered LUC activity was not identified for the combination of ZAT5 and the *PME58* promoter in transient expression analysis. These results suggest that ZAT5 suppresses the expression of *PME5*, *HMS*/*PME6*, *PME12*, and *PME16* rather than *PME58*. Our RNA-seq analyzes and qPCR results provide evidence that *PME58* expression increases in *zat5* mutants (Fig. 4A). Thus, ZAT5 may indirectly regulate the expression of *PME58*.

Published in : The Plant Cell (2024), vol. 36, n°10, pp. 4491–4510
DOI: 10.1093/plcell/koae209
Status : Postprint (Author's version)

Table 1. *Monosaccharide compositions of the nonadherent and AM layer obtained from WT, zat5-1, and zat5-2 seeds with water treatment*

Sugar	**Nonadherent mucilage (mg/g)**			**Adherent mucilage (mg/g)**		
	WT	***zat5-1***	***zat5-2***	**WT**	***zat5-1***	***zat5-2***
Mannose	0.9 ± 0.05	1.1±0.18	1.9 ± 0.26	0.6 ± 0.06	0.5±0.04	0.5±0.04
Rhamnose	12.6±0.33	12.1±0.79	12.0±1.12	6.1±0.19	6.2±0.10	6.2±0.16
GalA	17.2±0.08	16.9±0.02	17.3±0.18	7.7±0.10	7.5±0.47	7.3±0.32
Glucose	0.3±0.02	0.3±0.01	0.3±0.07	0.5±0.03	0.4 ±0.02	0.5±0.02
Galactose	0.3±0.01	0.3±0.04	0.4±0.02	0.7±0.01	0.7 ±0.02	0.7±0.01
Xylose	0.7±0.01	0.7±0.08	0.9±0.09	0.5±0.03	0.4±0.01	0.5±0.01
Arabinose	0.1±0.00	0.2±0.02	0.2±0.02	0.1±0.01	0.1±0.00	0.1±0.00
Fucose	...	...	...	...	...	...
Total	31.7±0.47	31.5±0.77	33.0±2.79	16.0±0.02	15.9±0.73	15.6±0.32
GalA/Rha (mol/mol)	1.2±0.03	1.2±0.04	1.2±0.11	1.1±0.03	1.0±0.06	1.0±0.03

The amount of sugar is presented as mean values (mg sugar g^{-1} seeds) ± SD of 3 independent samples. The results were not significantly different by Student's *t*-test. GalA, galacturonic acid; Rha, rhamnose.

Published in : The Plant Cell (2024), vol. 36, n°10, pp. 4491–4510
DOI: 10.1093/plcell/koae209
Status : Postprint (Author's version)

***Figure 3**. Zat5 decreased the DM of HG in seed mucilage.*

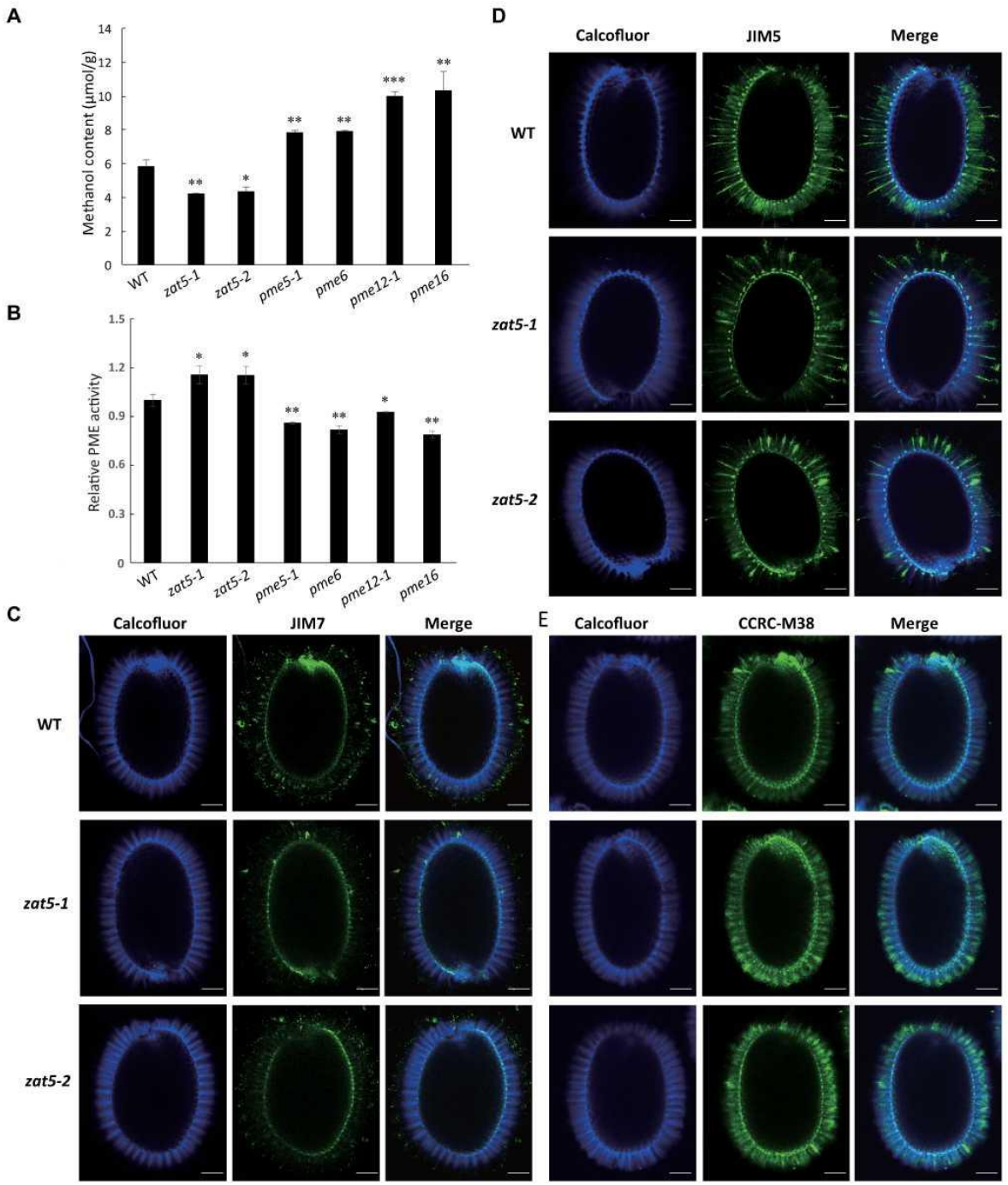

A) Methanol content released from the seed coat mucilage of WT, *zat5* and *pme5/6/12/16* mutants. Whole-seed mucilage was obtained by shaking seeds in water using the TissueLyser II (Qiagen) at 22 Hz. B) Relative PME activity in the developing seed coats of WT, *zat5*, and *pme5/6/12/16* mutants. Seed coats from 3 different batches of seed were used to extract total protein as biological repeats. The values were obtained by gel dispersion and standardized to the average PME activity of WT (=1). C to E) Immunolabeling of WT and *zat5* mutant seeds with JIM7 (C), JIM5 (D), and CCRC-M38 (E) monoclonal antibodies. Partially methylesterified HG is labeled with JIM7, lowly methylesterified HG is labeled with JIM5, and un-methylesterified HG is labeled with CCRC-M38. Bars = 50 µm. SD is shown with error bars (n = 3). Asterisks indicate significant differences compared with the WT (*P < 0.05, **P< 0.01, and ***P < 0.001) obtained using Student's t-test.

Published in : The Plant Cell (2024), vol. 36, n°10, pp. 4491–4510
DOI: 10.1093/plcell/koae209
Status : Postprint (Author's version)

Figure 4. *ZAT5 directly targets PME5, HMS/PME6, PME12, and PME16*

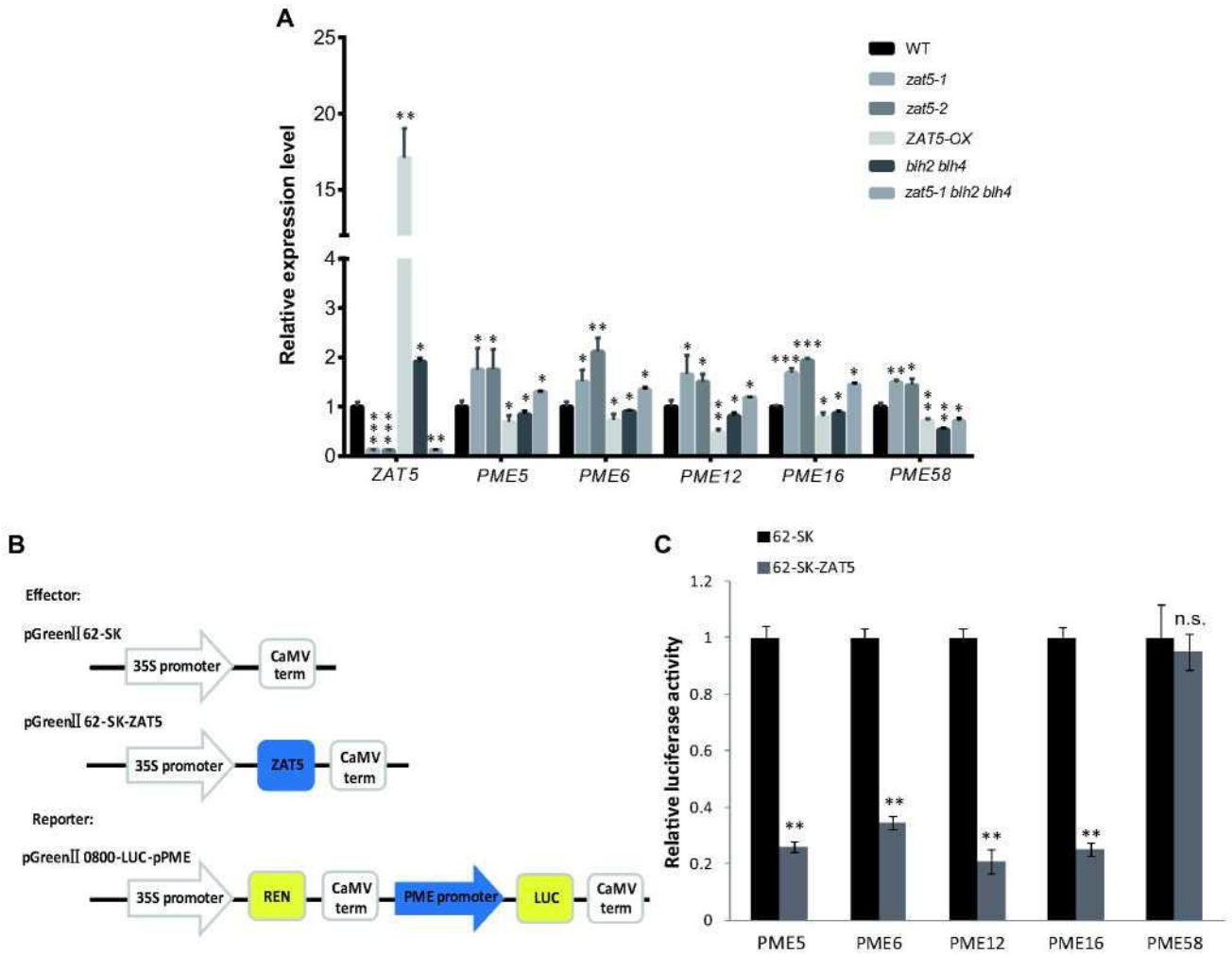

A) The relative expression of PME genes in 7 to 10 DPA seed coats from WT, *zat5-1*, *zat5-2*, *ZAT5* overexpressing plants, *blh2 blh4*, and *zat5-1 blh2 blh4*. Gene expression is shown relative to *ACTIN2*. The gene expression level in WT was set to 1. SD is shown with error bars (n = 3). Asterisks indicate significant differences compared with the WT (*P < 0.05, **P < 0.01, and ***P < 0.001) determined with Student's t-test. **B)** The vectors used in the dual-LUC assay including effectors and reporters. ZAT5 was introduced into the pGreenII 62-SK vector, and the promoters about 2,000 bp upstream of ATG in PME genes (*PME5*/*6*/*12*/*16*) were separately introduced into the pGreenII 0800-LUC vector. **C)** The relative LUC/REN ratios of the pGreenII 62-SK-ZAT5+pGreenII 0800-LUC-pPME and pGreenII 62-SK+pGreenII 0800-LUC-pPME) vector groups. SD is shown with error bars (n = 5). Asterisks indicate significant differences compared with the 62-sk control (n.s., not significant; ***P < 0.001) determined with Student's t-test.

ZAT5 RECOGNIZES TGATCA ELEMENTS IN VIVO AND IN VITRO

We performed a yeast one-hybrid (Y1H) assay to determine if ZAT5 binds to the promoters of *PME5*, *HMS*/*PME6*, *PME12*, and *PME16*. Our results indicate that ZAT5 binds to a genomic region ~2 kbp upstream of ATG in these genes (Fig. 5A).

A previous study has shown that AZF1/2/3 and ZAT10, which are homologs of ZAT5, bind to the A(G/C)T-$X_{3\text{-}4}$-A(G/C)T consensus sequence (Sakamoto et al. 2004). ZAT6 has been reported to positively regulate stress-related gene expression by binding to the TACAAT motif in their promoters (Shi et al. 2014).

Published in : The Plant Cell (2024), vol. 36, n°10, pp. 4491–4510
DOI: 10.1093/plcell/koae209
Status : Postprint (Author's version)

However, in preliminary experiments we found that ZAT5 did not recognize these motifs. Thus, to characterize the *cis*-elements that ZAT5 recognizes, the promoters of the 4 target genes of ZAT5 were analyzed using Plantcare (http://bioinformatics.psb.ugent.be/ webtools/plantcare/html/? tdsourcetag=s_pcqq_aiomsg) and MEME (https://meme-suite.org/meme/). A predicted TGATCA *cis*-element was identified. Our electrophoretic mobility shift assay (EMSA) experiments confirmed that maltose binding protein (MBP)-tagged ZAT5 (MBP-ZAT5) binds to the TGATCA repeat sequence but did not recognize the mutated probe (Fig. 5B). We then selected several sequences similar to the TGATCA motif in *PME5*, *HMS*/*PME6*, *PME12*, and *PME16* (Fig. 5C) and tested them with EMSA. These results suggested that MBP-ZAT5 directly bound to the promoter sequences of *PME5* (TGATGA), *HMS*/*PME6* (TGATCA), *PME12* (TGATCA), and *PME16* (TGAaTaCA) (Fig. 5, D to G). The binding can be eliminated with the addition of unlabeled competitors. By comparison, MBP-ZAT5 did not recognize the mutated version of the TGATCA motifs in these *PME* genes.

Published in : The Plant Cell (2024), vol. 36, n°10, pp. 4491–4510
DOI: 10.1093/plcell/koae209
Status : Postprint (Author's version)

***Figure 5**. ZAT5 directly targets PME5, HMS/PME6, PME12, and PME16.*

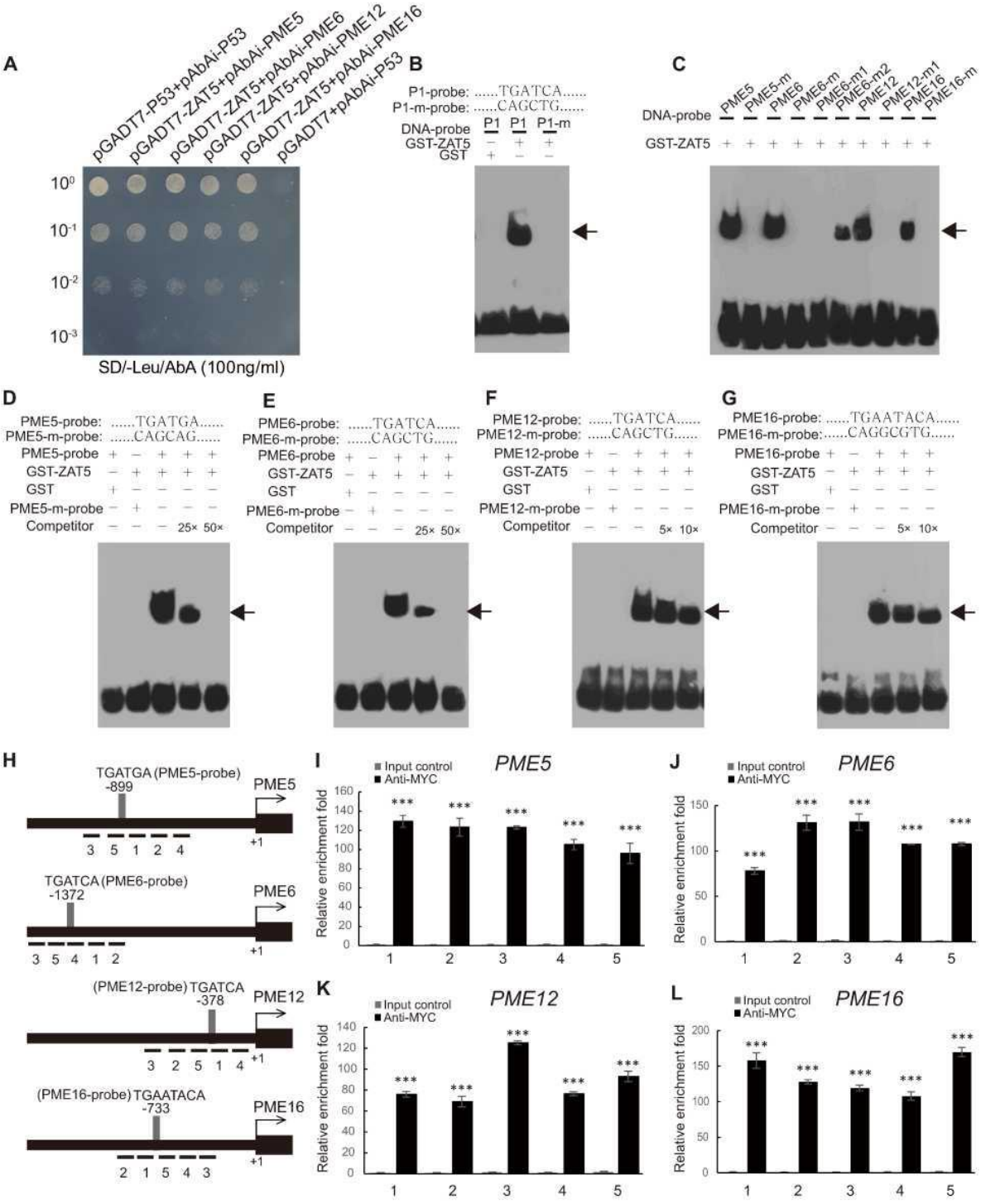

A) Yeast one-hybrid assays verified the interaction of ZAT5 with the ~2,000 bp upstream sequence of ATG in the *PME* promoters. B) EMSA demonstrating the binding of ZAT5 to TGATCA elements in vitro. P1 indicates the predicted binding site (TGATCA) of ZAT5. P1-m (CAGCTG) served as a negative control which was mutated from P1. C) EMSA showing the binding of ZAT5 to *PME5* (TGATGA), *HMS*/*PME6* (TGATCA), *PME6-m2* (TGATTG), *PME12* (TGATCA), and *PME16* (TGAATACA) in vitro. PME5-m (CAGCAG) was mutated from *PME5*, PME6-m (CAGCTG), and PME6-m1 (CAGCCA) were mutated from *PME6*, PME12-m1 (CAGCTG) was mutated from *PME12*, and PME16-m (CAGGCGTG) was mutated from *PME16*, which served as

Published in : The Plant Cell (2024), vol. 36, n°10, pp. 4491–4510
DOI: 10.1093/plcell/koae209
Status : Postprint (Author's version)

negative controls. D to G) EMSAs indicating the binding of ZAT5 to the TGATCA elements, respectively, in the promoters of *PME5* (D), *HMS*/*PME6* (E), *PME12* (F), and *PME16* (G). Competitors were unlabeled probes containing the same fragments. The corresponding mutated probes were used as negative controls. H) Various promoter positions in the candidate *PME*s genes examined by ChIP-qPCR (Lines 1 to 5). Gray bars represent possible conserved sequences examined by EMSA. The positions in the promoters are relative to the start codons of the *PME* genes. Numbers and bases represent the position and sequence information of ZAT5 binding to the promoter. I to L) ChIP-qPCR enrichment (fold) of ZAT5 binding to the *PME5* (I), *HMS*/*PME6* (J), *PME12* (K), and *PME16* (L) promoter regions. The ChIP experiment was performed with *proZAT5*:*ZAT5*:*zat5-MYC* transgenic Arabidopsis. Input genomic DNA was used as a negative control. SD is shown with error bars (n= 3). By using the Student's t-test, asterisks indicate significant differences compared with the input control (***$P < 0.001$).

We performed a chromatin immunoprecipitation (ChIP) experiment using 7 to 8 DPA developing seeds of WT and *proZAT5: ZAT5:zat5-MYC* transgenic plants to determine if ZAT5 directly regulates the *PME* genes in vivo. Five pairs of primers in the promoters of the *PME* genes were designed so that they could be detected by ChIP_qPCR (Fig. 5H). This analysis indicated that all the fragments in *PME* promoters were significantly enriched with MYC antibodies (Fig. 5, I to L), which suggest that ZAT5 is bound to these sequences in plants. These findings, together with our data showing that the expression of the target PME genes was upregulated in *zat5* mutants but downregulated in plants overexpressing *ZAT5* (Fig. 4A) led us to suspect that *PME5*, *HMS/ PME6*, *PME12*, and *PME16* expression is suppressed by binding of ZAT5 to TGATCA elements in their promoters.

GENETIC EVIDENCE THAT ZAT5 REGULATES PME5, HMS/ PME6, PME12, AND PME16 DIRECTLY

We have provided evidence that *PME5*, *HMS*/*PME6*, *PME12*, and *PME16* are negatively regulated by ZAT5. Previously, PME5 was reported to regulate pectin methylesterification during the development of phyllotaxis (Peaucelle et al. 2011). *HMS*/*PME6* is abundant in the embryo and seed coat, and is involved in embryo development. Mutating *HMS*/*PME6* was found to indirectly influence seed mucilage extrusion (Levesque-Tremblay et al. 2015a). *PME16* is expressed in the seed coat at 7 DPA, with a somewhat lower expression at 10 DPA (Levesque-Tremblay et al. 2015a). We used qPCR to determine the expression of these PME genes in developing seeds at 4 DPA and in seed coats at 7, 10, and 13 DPA. Our results showed that *PME5* and *PME16* were highly expressed in seed coats at 7 DPA compared to at 4 DPA. The expression of *PME6* reaches a maximum from 7 to 10 DPA and then decreases at 13 DPA. *PME12* expression was similar to, but a little lower than *PME6* expression (Supplementary Fig. S10).

To investigate if these PMEs are involved in seed mucilage development, we obtained T-DNA insert mutants for *PME5*, *HMS*/ *PME6*, *PME12*, and *PME16* from ABRC. RT-PCR confirmed that these mutants except *pme6* do not produce the WT transcript (Supplementary Fig. S11). The T-DNA insertion of *PME6* is located at -52 from the +1 site in the 5'untranslated region. RT-PCR results showed that the transcript levels of *HMS*/*PME6* in *pme6* were significantly lower than in WT (Supplementary Fig. S11). Thus, *pme6* is a knock-down mutant. RR staining of seeds that had been vigorously shaken in water showed that all *pme* mutants seem to have a thinner mucilage phenotype. Then, we measured the volume of both de-mucilaged seeds and seed mucilage. The results showed that the relative volume of de-mucilaged seeds have no significant difference

Published in : The Plant Cell (2024), vol. 36, n°10, pp. 4491–4510
DOI: 10.1093/plcell/koae209
Status : Postprint (Author's version)

(Supplementary Fig. S12), while the volume of AM layers of *pme* mutants decreased relative to WT (Fig. 6). To further examine the mucilage phenotype of these mutants, we crossed the *pme* mutants (female parent) and WT (male parent) to generate F1 seeds. The RR mucilage phenotype of the F1 seeds and the *pme* mutants were similar (Fig. 6). Thus, crosses of each *pme* mutant with WT suggest that the *pme* mucilage phenotype is a consequence of a seed coat defect.

We found that in the *pme5-1*, *pme6*, *pme12-1*, and *pme16* mutants the HG DM of mucilage was increased significantly and the PME activity in the 7 to 10 DPA seed coat was decreased compared to WT (Fig. 3, A and B). The intensity of immunolabeling *pme* seeds with JIM5 and JIM7 increased in the regions between ray structures and outer edges of the outer mucilage, respectively, whereas the labeling intensity of CCRC-M38 slightly decreased alongside the ray structure of AM layer compared with WT (Fig. 7; Supplementary Fig. S13). The quantitative results of ELISAs were consistent with the immunofluorescence results (Supplementary Fig. S14). Taken together, these results suggest that these PMEs are involved in seed mucilage pectin demethylesterification.

We next generated a series of double mutants (*zat5-1 pme5-1*, *zat5-1 pme6*, *zat5-1 pme12-1*, and *zat5-1 pme16*) and examined the phenotypes of their seed mucilage (Fig. 6). The thickness of the mucilage halo in these double mutants did not differ significantly from that of the WT. Thus, mutations of *PME5*, *HMS*/*PME6*, *PME12*, and *PME16* individually in the *zat5-1* mutant complement the *zat5* mucilage defect. Together, our genetic evidence indicates that ZAT5 regulates pectin demethylesterification by suppressing the expression of *PME5*, *HMS*/*PME6*, *PME12*, and *PME16* directly.

ZAT5 PHYSICALLY INTERACTS WITH BLH2 AND BLH4

In a previous study, we showed that BLH2 and BLH4 redundantly activate *PME58* expression to regulate pectin demethylesterification (Xu et al. 2020). ZAT5 may indirectly repress the expression of *PME58* according to our qPCR and dual-LUC activity data. These findings led us to investigate the relationship between ZAT5 and BLH2/4. qPCR was employed to detect *ZAT5* and *BLH2*/ *4* expression in the seed coats of *blh2/4* and *zat5* mutants, respectively. *ZAT5* expression was significantly increased in *blh2*, *blh4*, and *blh2 blh4*. *BLH2* and *BLH4* expression was increased in *zat5* mutants compared to the WT (Fig. 8A). Thus, ZAT5 and BLH2/4 may repress each other's transcription or prevent each other from acting normally.

A pull-down experiment was used to determine if there is an interaction between ZAT5 and BLH2 in vitro. MBP-ZAT5 was pulled down by the antiglutathione S-transferase (GST) antibodies when the purified glutathione S-transferase-tagged BLH2 fusion protein (GST-BLH2) reacted with MBP-tagged ZAT5 (Fig. 8B). GST alone did not pull-down MBP-ZAT5, suggesting that ZAT5 and BLH2 physically interact.

We then performed an in vivo co-immunoprecipitation (Co-IP) assay to confirm that ZAT5 and BLH2/4 interact. *Nicotiana ben- thamiana* leaves were used to separately co-express *Pro35S: MYC-ZAT5* with *Pro35S:BLH2-GFP* or *Pro35S:BLH4-GFP*. We then used anti-GFP antibodies to precipitate the protein complex. MYC-ZAT5 was immunoprecipitated in the presence of BLH2-GFP or BLH4-

Published in : The Plant Cell (2024), vol. 36, n°10, pp. 4491–4510
DOI: 10.1093/plcell/koae209
Status : Postprint (Author's version)

GFP but not with the GFP tag alone. This again indicates that in plant cells ZAT5 physically interacts with BLH2 and BLH4 (Fig. 8, C and D).

ZAT5 AND BLH2/4 ANTAGONISTICALLY REGULATE PECTIN DM

To determine if the interaction between ZAT5 and BLH2/4 affects the binding abilities of ZAT5 to *PME5*, *PME*6, *PME12*, and *PME16*, we performed EMSAs. Since BLH2 and BLH4 have a high amino acid sequence identity (58%) and are functionally redundant (Xu et al. 2020), we only used GST-BLH2 in these experiments. Biotin-labeled probes including the TGATCA core sequence were used to react with the purified GST-BLH2 and MBP-ZAT5 recombinant proteins. ZAT5 recognizes probes labeling TGATCA motifs of *PME5*, *PME*6, *PME*12, and *PME*16 (Fig. 8, E to H), while BLH2 does not (Fig. 8, E to H). However, adding increased amounts of the GST-BLH2 fusion protein did reduce the binding of ZAT5 to these probes (Fig. 8, E to H). Similarly, we also found that the binding of BLH2 to *PME58* was outcompeted by increasing the amounts of ZAT5 (Fig. 8I). These results suggest that ZAT5 and BLH2/4 inhibit each other's activities in a dose-dependent manner.

Published in : The Plant Cell (2024), vol. 36, n°10, pp. 4491–4510
DOI: 10.1093/plcell/koae209
Status : Postprint (Author's version)

***Figure 6**. Genetic analysis shows ZAT5 regulates PME5, 6, 12, and 16.*

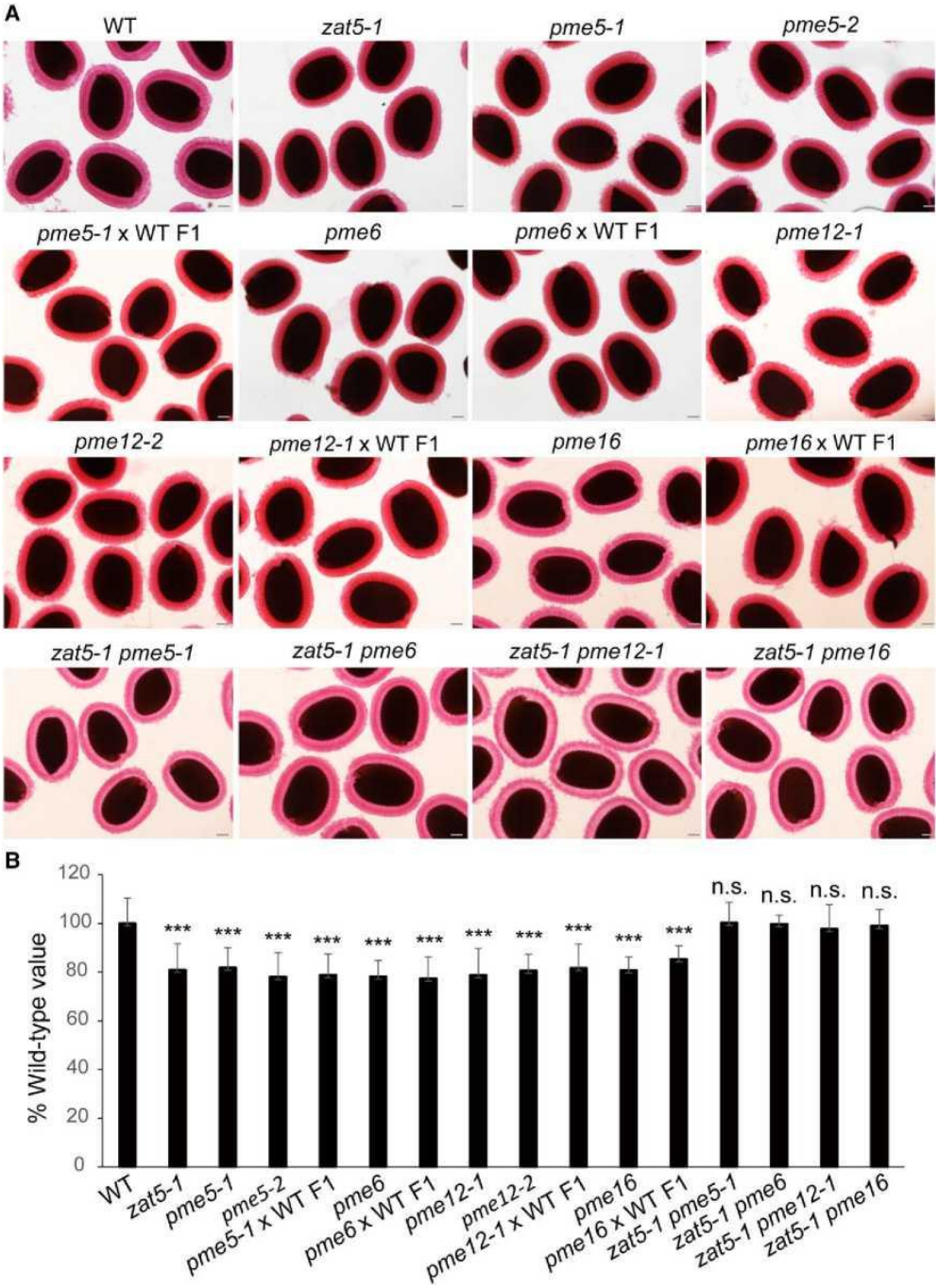

*A) The mucilage phenotypes of WT, zat5-1, F1 progeny of the cross between pme (female parent) and WT (male parent), and zat5-1 pme double mutant seeds. These seeds were stained with RR after shaking for 2 h at 200 rpm in water. Bars = 100 µm. B) The relative mucilage volume of AM layers. The average volume of WT seeds was set to 100%. SD is shown with error bars (n = 150 for WT and mutant seeds; n=60 for F1 hybrid seeds). Asterisks indicate significant differences compared with the WT (n.s., not significant; ***P < 0.001) obtained using the one-way ANOVA followed by Dunnett's multiple comparison test.*

Published in : The Plant Cell (2024), vol. 36, n°10, pp. 4491–4510
DOI: 10.1093/plcell/koae209
Status : Postprint (Author's version)

Our qPCR results suggest that *BLH2* expression was substantially elevated in *blh4*, whereas *BLH4* expression was significantly increased in *blh2* (Fig. 8A). These results are consistent with our previous finding that BLH2 and BLH4 work redundantly in the regulation of seed mucilage pectin methylesterification (Xu et al.

2020). To learn more about the relationship between ZAT5 and

BLH2/4 in regulating pectin DM, we crossed *zat5-1* with *blh2 blh4* to generate the *zat5-1 blh2 blh4* triple mutant. As shown in Fig. 9, A and B, *zat5-1* and *blh2 blh4* mutant seeds exhibited a clearly decreased mucilage layer compared to WT, while *zat5-1 blh2 blh4* showed a similar seed mucilage layer with *zat5-1*, thinner than WT. Notably, the seed mucilage layer of *zat5-1 blh2 blh4* was significantly thicker than that of *blh2 blh4*. Furthermore, the PME activity was decreased and HG DM was increased in the *zat5-1 blh2 blh4* triple mutant compared to in the WT, with levels between those in *zat5-1* and *blh2 blh4* (Fig. 9, C and D), suggesting that the *ZAT5* mutation could partially restore the phenotype deficiency in the *blh2 blh4* mutant. Additionally, *PME5*, *6*, *12*, *16*, and *58* had a compromised expression pattern in *zat5-1 blh2 blh4* compared to that in *zat5-1* and *blh2 blh4*, respectively (Fig. 4A). Above all, our findings imply that ZAT5 and BLH2/4 antagonize each other in regulating pectin DM in seed mucilage via the same route.

Figure 7. *Immunolabeling of pme5, pme6, pme12, and pme16 seeds with JIM5, JIM7, and CCRC-M38 monoclonal antibodies*

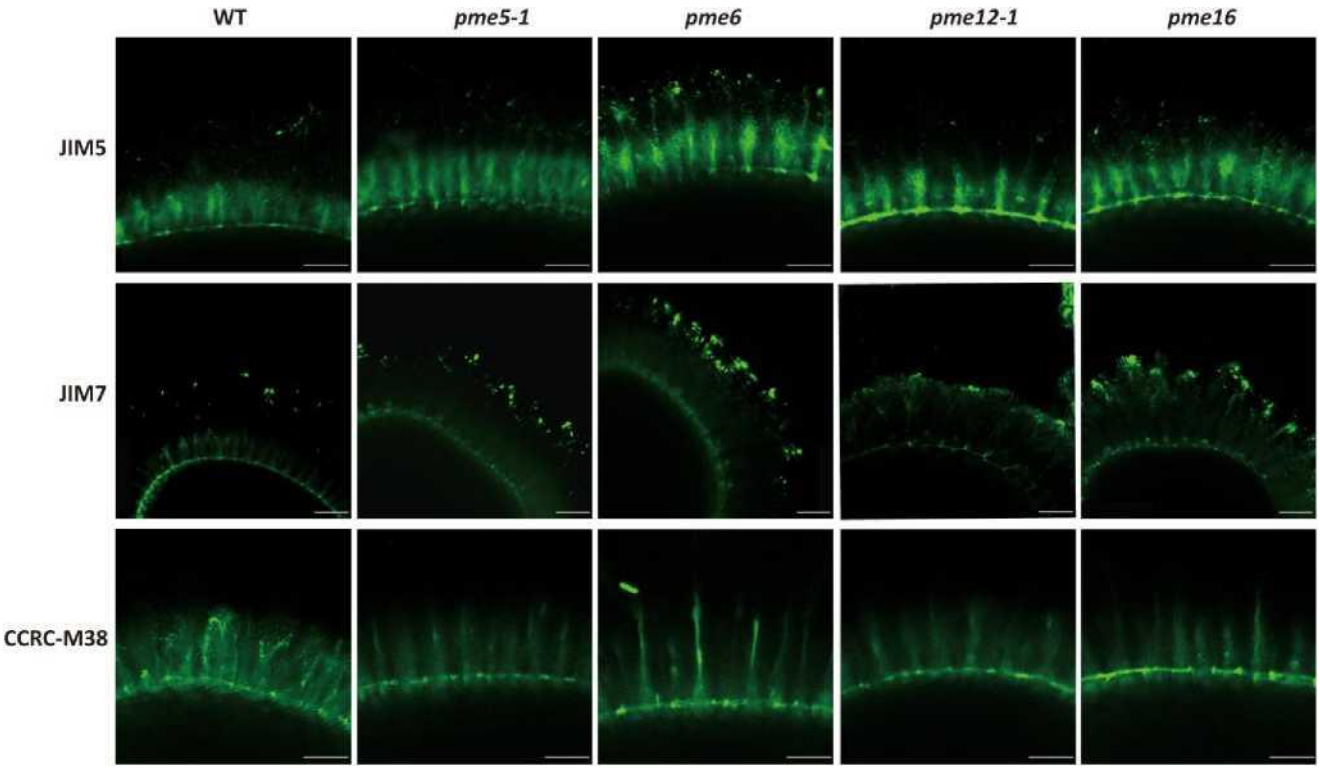

Lowly methylesterified HG is labeled with JIM5, partially methylesterified HG is labeled with JIM7, and un-methylesterified HG is labeled with CCRC-M38. Bars = 50 µm.

Published in : The Plant Cell (2024), vol. 36, n°10, pp. 4491–4510
DOI: 10.1093/plcell/koae209
Status : Postprint (Author's version)

Discussion

Pectin, as a highly complex polysaccharide abundant in plant primary cell walls, is an important factor in plant growth and has been shown to play roles in controlling cell elongation, cell adhesion, and cell wall porosity (Palin and Geitmann 2012; Levesque-Tremblay et al. 2015b; Saffer 2018; Wormit and Usadel 2018). The properties of the pectin networks are largely influenced by post-secretory changes due to the activity of pectin-modifying enzymes, including pectin methyl esterases (PMEs), pectin methylesterase inhibitors (PMEIs), and pectin-degrading enzymes (Senechal et al. 2014; Wormit and Usadel 2018). For example, HG is the most abundant component of pectin and is typically deposited into the cell wall in a highly methylesterified form (Wolf et al. 2009). PMEs catalyze the demethylesterification of these HGs and their activity is regulated by PMEIs (Wolf et al. 2009; Senechal et al. 2014). Nevertheless, little has been reported on the molecular regulatory mechanisms of pectin demethylesterification.

The seed coat mucilage of *Arabidopsis* has become a valuable model system for studying the production, modification, and interaction of polysaccharides, especially pectin (Sola et al. 2019). Using the seed coat mucilage system, several transcription factors including BLH2/4, ERF4, LUH/MUM1, MYB52, and STK have been shown to regulate HG demethylesterification. While most of these regulators do this by regulating *PMEI*-related genes, only BLH2 and BLH4 were reported to regulate HG demethylesterification by directly activating *PME58* (Xu et al. 2020). Using this system, we have provided evidence that ZAT5, a C2H2-type ZFP, negatively regulates demethylesterification of pectin in seed coat mucilage by repressing 4 PME genes, including *PME5*, *HMS*/*PME6*, *PME12*, and *PME16*. Furthermore, we found that ZAT5 regulates these PME genes by binding to the TGATCA *cis*-element in their promoters, and no other C2H2 transcription factors have been reported to recognize this *cis*-element (Fig. 5).

It is interesting to note that ZAT5 and BLH2/4 interact with each other, which represses their respective abilities to transcriptionally regulate target genes. Based on our data, we have developed a model describing how the ZAT5-BLH2/4 interaction modulates pectin demethylesterification (Fig. 10). ZAT5 directly represses the expression of *PME5*, *6*, *12*, and *16* by binding to their TGATCA motif and indirectly represses *PME58* by antagonizing BLH2/4. This leads to a negative regulation of pectin demethylesterification. *PME5*, *6*, *12*, and *16*, are unlikely to be direct targets of BLH2/4 since their promoters contain no TGACAGGT motif. BLH2/4 activates *PME58* by directly binding to its promoter and regulate *PME5*, *6*, *12*, and *16* expression indirectly by suppressing ZAT5 activity. This results in a positive regulation of pectin demethylesterification. In summary, our studies reveal that ZAT5 and BLH2/4 antagonistically modulate downstream genes to control the levels of pectin methylesterification in the *Arabidopsis* seed coat.

Published in : The Plant Cell (2024), vol. 36, n°10, pp. 4491–4510
DOI: 10.1093/plcell/koae209
Status : Postprint (Author's version)

***Figure 8**. ZAT5 and BLH2/4 are functionally antagonistic to each other in regulating downstream genes expression.*

A) *ZAT5*, *BLH2*, and *BLH4* expression patterns in 7 to 10 DPA seed coats of WT, *zat5-1*, *zat5-2*, *blh2*, *blh4*, and *blh2 blh4*.

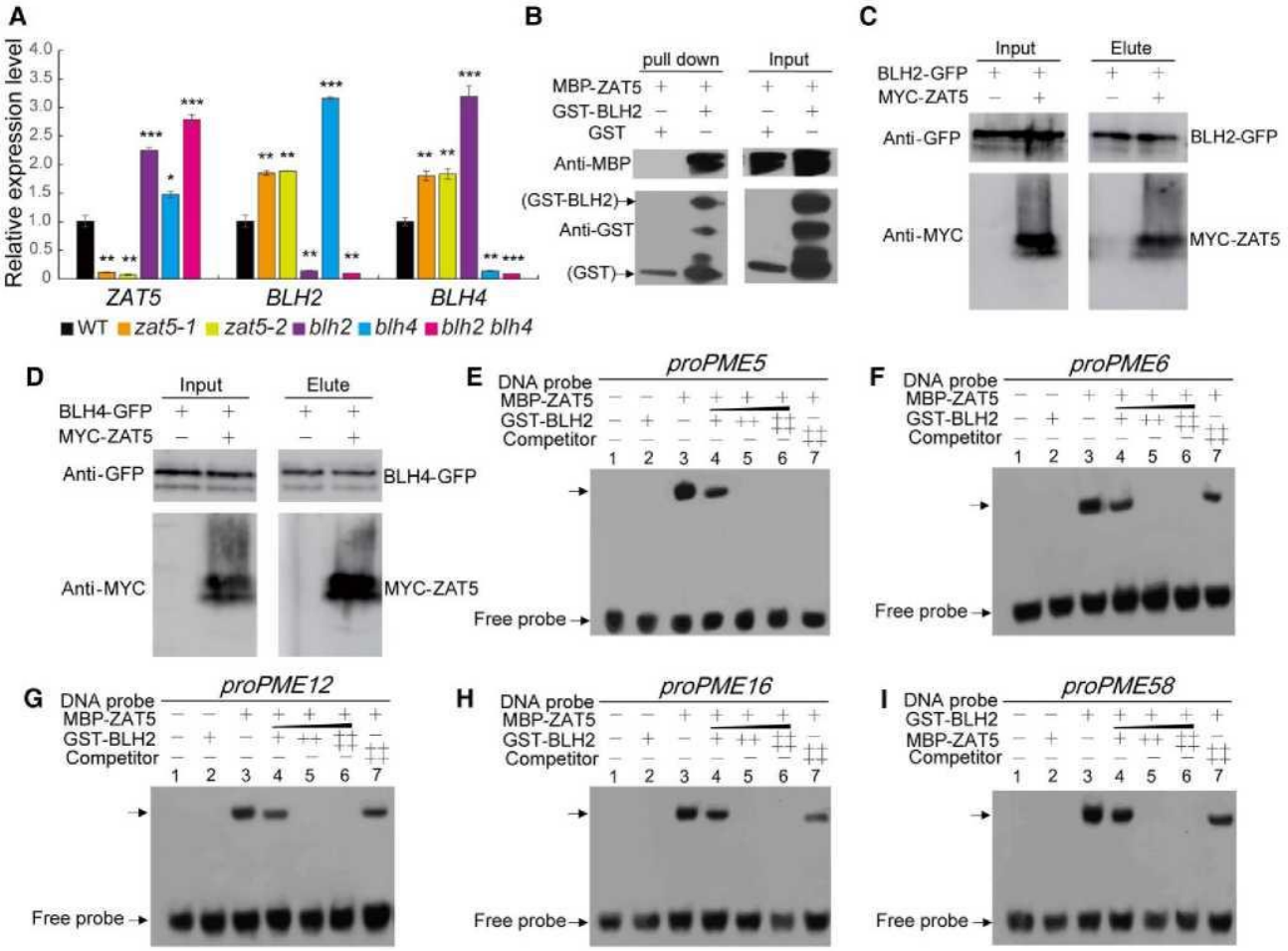

Gene expression is shown relative to *ACTIN2*. The expression level in WT was set to 1. SD is shown with error bars ($n = 3$). Asterisks indicate significant differences compared with the WT (*$P < 0.05$, **$P < 0.01$, and ***$P < 0.001$) obtained using Student's *t* -test. B) ZAT5-BLH2 interaction examined by a pull-down assay. The MBP-ZAT5 fusion protein was reacted with the GST-BLH2 fusion protein or GST. The anti-GST antibodies pulled down MBP-ZAT5 but not MBP, reacted with GST-BLH2. C and D) Co-IP test of ZAT5 and BLH2/4 interaction in vivo. *Nicotiana benthamiana* leaves were used to co-express MYC-ZAT5 with BLH2-GFP (C), BLH4-GFP (D), or the GFP tag alone. IP was performed using an anti-GFP antibody. An immunoblot with anti-MYC antibody was used to label MYC-ZAT5 and indicates that there is a physical interaction between ZAT5 and BLH2 (C), as well as ZAT5 and BLH4 (D). E to H) EMSA reveals that ZAT5's ability to bind to DNA is diminished in the presence of BLH2. ZAT5 (Lane 3) attaches to probes with TGATCA motifs from *PME5* (E), *PME6* (F), *PME12* (G), and *PME16* (H), whereas BLH2 (Lane 2) did not bind to these motifs. Increasing the amounts of GST-BLH2 decreases the binding of ZAT5 to these promoters (Lanes 4 to 6). The fusion proteins MBP-ZAT5 and GST-BLH2 were purified. I) EMSA indicating that ZAT5 interferes with BLH2's capacity to bind *PME58*. ZAT5 (Lane 2) did not recognize the TGACAGGT motif of the *PME58* promoter, but BLH2 (Lane 3) did bind to it. ZAT5 prevented BLH2 from binding to these probes containing the TGACAGGT motif (Lanes 4 to 6). The DNA probes were 5′-biotin-labeled. Competitors had the same fragments but were not labeled.

Published in : The Plant Cell (2024), vol. 36, n°10, pp. 4491–4510
DOI: 10.1093/plcell/koae209
Status : Postprint (Author's version)

In this work, we have shown that ZAT5 is a repressor of HG de- methylesterification, similar to MYB52. In *myb52* mutants, there is a relocation of mucilage between the NM and AM layers but this is not observed in *zat5* mutants (Table 1; Supplementary Fig. S7). Nevertheless, in *zat5* mutants, there was a change in the degree/ pattern of HG methylesterification which may alter the compactness of the mucilage and increase the strength of the pectin gel matrix, leading to a thinner mucilage layer (Fig. 2). The large number of plant PME and PMEI isoforms is believed to reflect their diverse roles in modifying cell wall pectin during growth and development (Wormit and Usadel 2018). Different patterns of pectin demethylesterification, such as blockwise and linear demethylesterification, exert distinct effects on pectin properties. In blockwise demethylesterification, clusters of contiguous methylester groups are removed from the pectin chain, creating regions with high degrees of de-esterification. This pattern can lead to the formation of "egg-box" structures, enhancing pectin gelation and strengthening cell wall integrity (Hocq et al. 2017). On the other hand, linear demethylesterification results in a more uniform distribution of de-esterified regions along the pectin chain. This pattern may promote interactions with calcium ions more evenly throughout the molecule, influencing gelation kinetics and rheological properties. The differential effects of these demethylesterification patterns highlight the complexity of pectin structure-function relationships and underscore the importance of understanding their implications for various applications, from food texture modification to plant cell wall mechanics (Willats et al. 2001; Wormit and Usadel 2018). Thus, we speculate that the PMEs and PMEIs that are regulated by ZAT5 and MYB52 may control different patterns and degrees of HG demethylesterifica- tion and thereby affect the physical properties of seed mucilage differently.

Figure 9. *ZAT5 and BLH2/4 antagonize each other in regulating pectin DM*

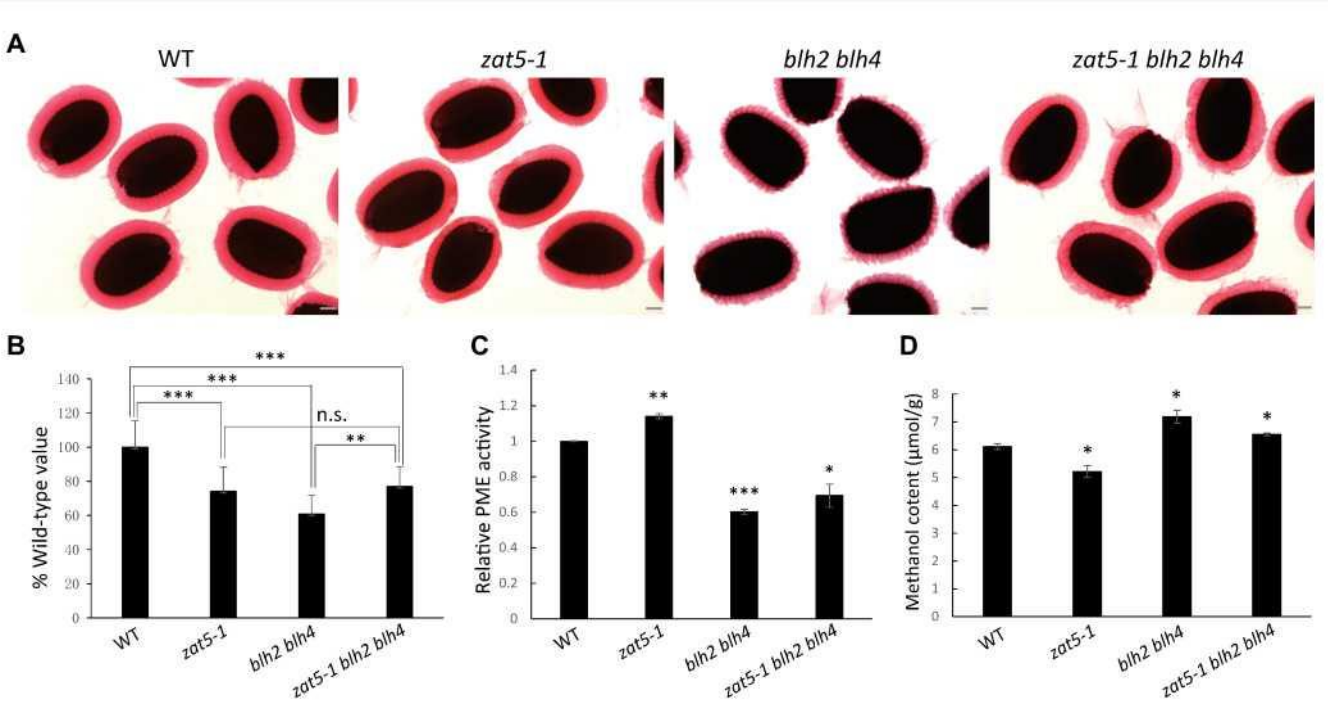

Published in : The Plant Cell (2024), vol. 36, n°10, pp. 4491–4510
DOI: 10.1093/plcell/koae209
Status : Postprint (Author's version)

A) Mucilage phenotypes of WT, *zat5-1*, *blh2 blh4*, *zat5-1 blh2 blh4* revealed after seeds were shaken for 2 h at 200 rpm in water. Scale bars = 100 µm. B) The relative mucilage thickness of AM layers. The WT seeds' average thickness was set to 100%. Error bars indicate SD (*n*= 150). Asterisks indicate significant differences compared with the WT by the one-way ANOVA followed by Tukey's multiple comparison test (n.s., not significant; ***P*< 0.01 and ****P* < 0.001). C) Relative PME activity of *zat5-1, blh2 blh4, zat5-1 blh2 blh4* mutants compared with WT. The values were determined using a gel diffusion assay and were normalized to the average WT activity (=1). Total protein was extracted from three different batches of seed coats as biological replicates. Error bars indicate SD (*n* = 3). Asterisks indicate significant differences compared with the WT by the Student's *t*-test (**P* < 0.05; ***P* < 0.01, and ****P* < 0.001). D) Methanol content released from the whole mucilage of WT, *zat5-1, blh2 blh4, zat5-1 blh2 blh4* mutants. Whole mucilage was extracted by shaking seeds in water on the TissueLyser II (Qiagen) at 22 Hz. Error bars indicate SD (*n* = 3). Asterisks indicate significant differences compared with the WT by the Student's *t*-test (**P* < 0.05).

Figure 10. *Models depicting the regulatory networks of ZAT5 and BLH2/4 involved in HG demethylesterification of Arabidopsis seed coat.*

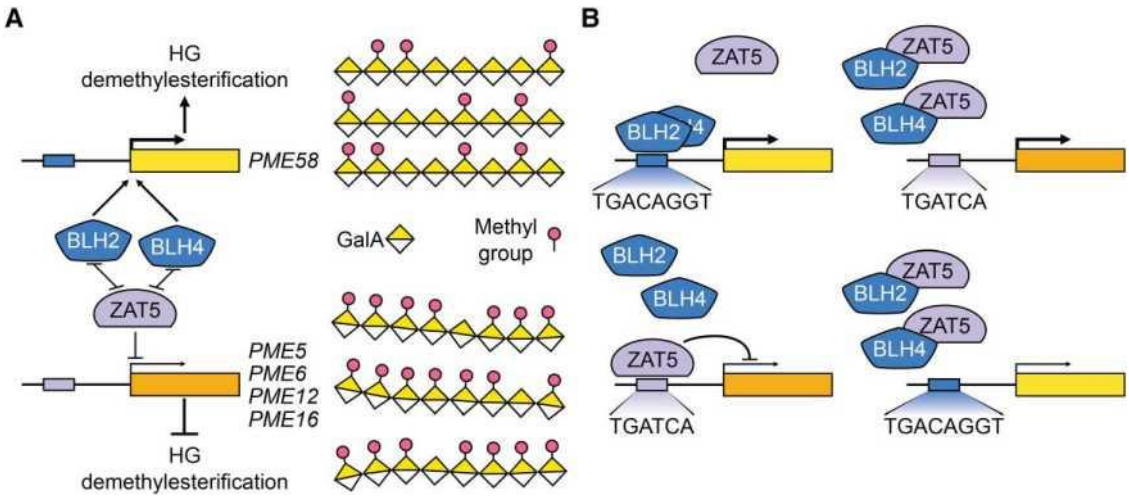

A) The role of ZAT5 and BLH2/4 in HG demethylesterification of seed coat in *Arabidopsis* (Xu et al. 2020). B) ZAT5 and BLH2/4 regulate target genes encoding PMEs by repressing each other's activity. ZAT5 increases HG DM by inhibiting *PME5/6/12/16* expression and indirectly inhibiting *PME58* expression by limiting the binding of BLH2/4 to the *PME58* promoter. BLH2/4 decreases HG DM by activating *PME58*, and indirectly activating *PME5*, *PME6*, *PME12*, and *PME16* by preventing ZAT5 from binding to their promoters.

The cell wall is the first barrier in a plant's response to environmental stresses. The level of cell wall pectin methylesterification regulated by PME/PMEI activity is believed to have an important role in defense against microbial pathogens and viruses (Senechal et al. 2014; Wormit and Usadel 2018). Other studies have shown that PMEs and PMEIs may contribute to plant responses to drought, salt, and extreme temperature, although the underlying mechanisms are largely unclear (Kumar et al. 2023). In addition to its expression in seeds, *HMS*/*PME6* is expressed in guard cells where it is required for normal stomatal function through modulating pectin methylesterification in the guard cell wall (Amsbury et al. 2016). Stomata consist of guard cells which conduct environmental or stress signals to induce various endogenous responses for adaptation to environmental changes (Liu and Xue 2021). The ability of ZAT5 to regulate pectin demethylesterification could be associated with stress resistance. Indeed, most members of the C1-2i subclass including AZF1, AZF2, AZF3, ZAT6, ZAT7, ZAT10, ZAT11, ZAT12, and ZAT18, have been shown to be involved in

Published in : The Plant Cell (2024), vol. 36, n°10, pp. 4491–4510
DOI: 10.1093/plcell/koae209
Status : Postprint (Author's version)

various stress responses, including drought (Sakamoto et al. 2000, 2004; Yin et al. 2017), salt (Sakamoto et al. 2004), cold (Jaglo et al. 2001; Vogel et al. 2005), osmotic (Desikan et al. 2001; Davletova et al. 2005; Qureshi et al. 2013), and pathogen stress (Shi et al. 2014). Thus, it will be interesting to further study whether these ZAT5 homologs are involved in the stress response by regulating PME genes.

To date, only a few PME genes have been demonstrated to influence seed coat mucilage formation. In our study, we found evidence suggesting that PME5, HMS/PME6, PME12, and PME16 may play roles in seed mucilage metabolism, with expression of their genes regulated by ZAT5. Levesque-Tremblay et al. (2015a) identified several PME genes expressed in the seed coat. Among the six *pme* mutants obtained, namely *hms-1*, *pme7*, *pme19*, *pme42*, *pme44*, and *pme58*, only the *hms-1* mutant exhibited a deficiency in mucilage extrusion after RR staining (Levesque-Tremblay et al. 2015a). Our study revealed that *pme* mutants (*pme5*, *pme6*, *pme12*, and *pme16*) exhibited defects in mucilage thickness, which may be easily overlooked without quantification (Fig. 6). Furthermore, the *pme6* mutant obtained in our study is a knock-down mutant (Supplementary Fig. S11), differing from the *hms-1* mutant, which lacks the WT transcript of *HMS*/*PME6* entirely (Levesque-Tremblay et al. 2015a). Specifically, *pme6* displayed normal embryo morphology but exhibited a thinner adherent layer and decreased PME activity (Figs. 3 and 6). In contrast, the *hms-1* mutant displayed abnormalities in embryo development in addition to defects in mucilage extrusion and altered PME activity. The milder phenotype observed in *pme6* compared to *hms-1* may be attributed to the presence of residual *HMS*/*PME6* transcripts in *pme6*. *ZAT5* is highly expressed in the seed coat, CZSC, embryo, and endosperm (Fig. 1), and its effects on the mucilage phenotype are unclear. Considering the spatial complexity of plant regulatory mechanisms, ZAT5 may be involved in seed mucilage modification by affecting other, as yet unknown, steps of seed development.

In all, PME function requires precise regulation as its activity substantially impacts various aspects of plant physiology and development (Wolf et al. 2009). Fine-tuning PME activity is crucial for maintaining optimal cell wall integrity (Wolf et al. 2012), controlling fruit texture and ripening processes (Xue et al. 2020), modulating cell expansion (Jiang et al. 2005), and regulating responses to environmental stresses and pathogens (Volpi et al. 2011). Imbalances in PME activity can lead to detrimental effects such as altered fruit quality, compromised resistance to pathogens, and impaired growth. Therefore, precise regulation of PME activity is essential for ensuring proper plant growth, development, and adaptation to changing environmental conditions (Pelloux et al. 2007; Wu et al. 2018). Our discovery of the antagonistic regulation between ZAT5 and BLH factors sheds light on the intricate control of pectin demethylesterification, highlighting the critical importance of pectin demethylesterification in orchestrating various aspects of plant physiology and adaptation.

Published in : The Plant Cell (2024), vol. 36, n°10, pp. 4491–4510
DOI: 10.1093/plcell/koae209
Status : Postprint (Author's version)

Materials and methods

PLANT MATERIALS AND PLANT GROWTH

Arabidopsis (*A. thaliana*) Columbia-0 (Col-0) was used as the control. T-DNA insertion mutants including *zat5-1* (SAIL_13_H11),

zat5-2 (SALK_048250), *pme5-1* (SALK_145314), *pme5-2* (Sail_184_F04), *pme6* (SALKseq_038198), *pme12-1* (SALK_048655) (Bethke et al. 2014), *pme12-2* (SALK_058895C) (Bethke et al. 2014), *pme16* (SAILseq_409_B10), *blh2-1* (SALK_009120) (Xu et al. 2020), and *blh4-1* (SALK_121117) (Xu et al. 2020) were purchased from the Arabidopsis Biological Resource Center (http://www.arabidopsis.org). Homozygous lines were identified by RT-PCR genotyping with appropriate primers (Supplementary Table S1).

Seeds were surface sterilized with aq. 75% (*v*/*v*) ethanol and then washed 3 times with sterile distilled water. The seeds were sown on half-strength Murashige and Skoog (MS) medium, stratified for 3 d at 4 °C in the absence of light, and then germinated at 20 to 22 °C under a 16 h/8 h light/dark photoperiod with a light intensity of 110 mmol m^{-2} s^{-1} and relative humidity of 60%. Seedlings were transferred to soil after 7 d and grown in the same environment. Screening for transformed plants was performed with half-strength MS medium containing hygromycin (20 mg/L) or kanamycin (50 mg/L). Antibiotic-resistant seedlings were transplanted into soil and grown at 20 to 22 °C under a 16 h/8 h light/dark photoperiod with a light intensity of 110 mmol m^{-2} s^{-2} and relative humidity of 60%. Double or triple mutants were generated by crossing *zat5-1* with *pme5*, *pme6*, *pme12*, *pme16* single mutants or with *blh2 blh4* double mutants.

GENE EXPRESSION ANALYSIS AND GUS STAINING ASSAY

Seven to 10 DPA developing seeds from at least 100 siliques were collected and spread on glass slides (Xu et al. 2020). The embryos and most of the endosperm were forced out by squeezing the seeds with another slide. The seed coats were then collected and frozen in liquid nitrogen. Three different batches of developing seeds were harvested as biological replicates from WT, *zat5-1*, *zat5-2*, *pme5*, *pme6*, *pme12*, *pme16*, *blh2*, *blh4*, *blh2 blh4*, *zat5-1 blh2 blh4*, and *Pro35S:ZAT5*. The seeds or seed coats from the same batch were obtained from at least 50 plants for each replicate. Tissues were frozen in liquid nitrogen and total RNA then extracted using the Transgene Plant RNA Kit (Transgene, ER301-01). First-strand cDNA from RNA was prepared using Transgene One-Step gDNA Removal and cDNA Synthesis SuperMix (Transgene, AE311-02). RT-PCR was performed using a Veriti 96-Well Thermo Cycler (Applied Biosystems, Thermo Fisher Scientific) with *ACTIN2* as reference. qPCR was performed using an ABI 7500 real-time PCR system (Applied Biosystems, Carlsbad, CA, USA) with *ACTIN2* as control. Data were obtained using the $2^{-\Delta\Delta Ct}$ method (Livak and Schmittgen 2001). Student's *t*-tests were used to compare expression levels. The primers used are listed in Supplementary Table S2.

A ~2,014 bp DNA fragment upstream from the ATG of *ZAT5* was cloned by PCR using appropriate

Published in : The Plant Cell (2024), vol. 36, n°10, pp. 4491–4510
DOI: 10.1093/plcell/koae209
Status : Postprint (Author's version)

primers (Supplementary Table S3). The PCR products were inserted into the pCAMBIA1301 binary vector with Pst I and Nco I sites to generate *ProZAT5:GUS*. The constructs were then introduced into WT plants by *Agrobacterium tumefaciens*-mediated transformation. Homozygous T3 plants were employed for further analysis. A histochemical GUS assay was performed using the GUS staining kit (Coolaber Manufacturer) according to the manufacturer's instructions. Briefly, the tissues were immersed in GUS staining solution and kept overnight at 37 ° C. The tissues were then decolorized with aq. 70% (*v*/*v*) ethanol. GUS signal was observed under white light and photographed using a MDG29 stereoscopic microscope (LEICA).

SEED STAINING AND DETERMINATION OF AM VOLUMES

Mucilage phenotypes were characterized after shaking mature dry seeds in deionized water for 2 h at 28 °C and 200 rpm, by

staining for 30 min with aq. 0.01% (*w*/*v*) RR (Solarbio). The seeds were then gently washed several times with water and photographed using a bright-field microscope (SZX16; Olympus). A protocol adapted from Xu et al. (2022) was used to determine AM volumes by the ImageJ 1.34S software. Three batches of seeds collected from more than 30 plants were regarded as bioreplicates for WT and mutants. Around 150 seeds were analyzed to determine the volume of de-mucilaged seeds and AM. For F1 generation, more than 60 seeds were analyzed. The length (2a) and width (2b) of each seed, as well as the length (2A) and width (2B) of the same seed plus AM were measured. The volume of AM was calculated by subtracting the volume of the seed ($V = 4/3^* \pi * a * b * b$) from the volume of seed plus mucilage halo ($V = 4/3 * \pi * A * B * B$).

PLASMID CONSTRUCTION AND PLANT TRANSFORMATION

The *ZAT5* full-length CDS was isolated and inserted into pCAMBIA35tlegfps2#4 to generate *Pro35s:ZAT5* overexpressing vectors. The *ZAT5* promoter region (2,014 bp upstream of ATG) and the *ZAT5* full-length CDS were individually cloned and introduced into a MYC-tagged pCAMBIA1300 binary vector to obtain *proZAT5:MYC-ZAT5*. The vectors were then introduced into *Arabidopsis* Col-0 or the *zat5-1* mutant using the *Agrobacterium* GV3301 mediated floral dip method (Clough and Bent 1998). Transformants were identified by growth on 1/2 MS medium, containing kanamycin (50 mg/L) or hygromycin (20 mg/L). The related primers are listed in Supplementary Table S3. T2 or T3 generation transgenic lines were used for subsequent analyzes.

MONOSACCHARIDE COMPOSITION ANALYSIS

Seed coat mucilage was extracted from 20 mg of mature dry seeds. The NM layer was extracted with 2 mL of deionized water [or 50 mM EDTA; EDTA extracts are dialyzed with running deionized water for at least 24 h (molecular weight cut off 3,500)] by shaking for 2 h at 200 rpm, and the supernatant was obtained after a short centrifugation. The AM was obtained by ultrasonic treatment (Zhao et al. 2017). All the samples were vacuum dried. Then, the NM and AM mucilage samples were hydrolyzed for 2 h at 121 °C with 0.5 mL of 2 M trifluoroacetic acid. The solutions

Published in : The Plant Cell (2024), vol. 36, n°10, pp. 4491–4510
DOI: 10.1093/plcell/koae209
Status : Postprint (Author's version)

were concentrated to dryness at 60 °C under a stream of nitrogen gas. The released monosaccharides were derivatized by treatment for 30 min at 70 °C with 0.5 mL 1-phenyl-3-methyl-5-pyrazolone (PMP) and 0.5 mL 0.3 M NaOH. Chloroform was added and the aqueous phase collected and then washed with chloroform. The PMP-derivatized monosaccharides in the aqueous phase were then quantified using a Waters HPLC system with a Hypersic ODS-2 C18 column (4.6 x 250 mm; Thermo Scientific, USA) (Shi et al. 2018). An equimolar mixture of arabinose (Ara), fucose (Fuc), galactose (Gal), galacturonic acid (GalA), glucose (Glc), rhamnose (Rha), mannose (Man), and xylose (Xyl), which had been treated the same as the mucilage was used as standard.

IN SITU HYBRIDIZATION

The protocol used here was previously described (Hu et al. 2016). Seeds from four developmental stages (4, 7, 10, and 13 DPA) were fixed, dehydrated, embedded, sectioned, and attached to adhesive slides. Digoxigenin-labeled probes were generated by cloning the coding region of *ZAT5* with specific primers and ligating it to the pGM-T vector. An in vitro transcription kit (Roche) was used to generate digoxigenin-labeled sense and antisense RNA probes with either the T7 or the SP6 promoters. The blocking reagent, Nitro-blue tetrazolium/5-bromo-4-chloro-3-indolylphosphate stock solution, and antidigoxigenin antibody used for hybridization were

obtained from Roche. Antisense and sense samples were run in parallel. The images were obtained using an Olympus light microscope.

IMMUNOLABELING

Whole-seed immunolabeling was performed as described by Xu et al. (2020). We first blocked at least 20 mature dry seeds with defatted milk powder [3% *w*/*v* in phosphate-buffered saline (PBS)]. The seeds were washed 3 times with PBS, and then reacted for 1 h at 37 °C with the primary monoclonal antibodies (JIM5, JIM7, and CCRC-M38) which had been diluted 10-fold with blocking solution. The seeds were washed with PBS and kept for 1.5 h at 37 °C in the absence of light with AlexaFluor488-tagged donkey antirat IgG (Thermo Fisher Scientific) for JIM5 and JIM7 or a donkey antimouse IgG (Thermo Fisher Scientific) for CCRC-M38. The AlexaFluor488-tagged antibodies were diluted 200-fold with blocking solution. The labeled seeds were then stained for 15 min with Calcofluor White diluted 1:5 in PBS, and washed with PBS several times. A FluoView Fv1000 confocal microscope (Olympus) was used to capture images. Calcofluor and AlexaFluor488 were excited with a 405 nm diode laser and a 488 nm argon laser, respectively. Fluorescence emission was recorded between 410 and 500 nm for Calcofluor and between 500 and 630 nm for Alexa Fluor488. For image acquisition within each experiment, the same settings were employed.

ELISA was performed with a similar method as previously described (Yu et al. 2014). The AM extractions were coated onto the microtiter plates (Costa 3599) with a concentration of 50 to 100 µg/mL. The plates were washed with PBS and 200 µL of 3% (*w*/*v*) milk protein in phosphate-buffered saline (MP/PBS) was added to block the plates for 2 h at room temperature. After washing with PBS, 100 µL per well of the primary antibody with a 25-fold dilution in MP/PBS was added.

Published in : The Plant Cell (2024), vol. 36, n°10, pp. 4491–4510
DOI: 10.1093/plcell/koae209
Status : Postprint (Author's version)

After 2 h of incubation at 37 °C and washing with PBS, the wells were incubated with antirat/anti-mouse IgG coupled to horseradish PRX at a 1,000-fold dilution in MP/PBS for another 2 h. After washing with PBS, the antibody binding was determined by adding 150 μL per well of horseradish PRX-substrate (tetramethylbenzidine liquid substrate, Sigma T0440). The reaction was stopped after 5 min by adding 50 µL per well of 1 N sulfuric acid. The absorbance was measured at 450 nm in a microplate reader.

DETERMINATION OF PECTIN DM AND PECTIN ACTIVITY

The amount of methanol released from seed mucilage was used to determine the DM in WT and mutants. Three different batches of seeds from at least 50 plants were used. Mucilage was solubilized from mature seeds (20 mg) by vigorous shaking for 1 h in 500 µL water using a TissueLyser II (Qiaqen) at 22 HZ. A portion of the supernatant (200 µL) was saponified for 1 h by adding NaOH (28 µL, 2 M) on an orbital shaker. The solution was neutralized with 28 µL HCl (2 M) and centrifuged for 10 min at 10,000 x *g*. Alcohol oxidase (Solarbio, A6850) was then added and the mixture kept for 15 min at 25 °C. 2,4-Acetylacetone (100 ^L 0.02 M) was added and allowed to react for 15 min at 60 °C. The A_{412nm} was then measured. The amount of released methanol was determined as described.

A previously described method was used to determine PME activity (Ding et al. 2021). The seed coats were separated from at least 100 developing siliques at 7 to 10 DPA and used to extract protein. Developing seeds from 3 separate batches of plants were used as biological duplicates. Total proteins were obtained using the One Step Plant Active Protein Extraction Kit (Sangon Biotech). Protein concentrations were determined using the Bradford method (Bradford 1976). The gels used for quantification

of PME activity was composed of 0.1% (*w*/*v*) citrus fruit pectin (>85% esterified; Sigma-Aldrich) in 50 mM Na_2HPO_4, pH 6.5 containing 12.5 mM citric acid. The gels were heated and then cooled in the mold. Wells (6-mm diameter) were cut in gels and then 10 mg protein was added and kept overnight at 28 °C. The gels were stained for 1 h with mild rotation using 0.01% (*v*/*v*) RR, and then washed with water several times. The area of the red-stained region was calculated using Image J 1.34S. The relative PME activity was standardized by setting the average area of WT to 1.

RNA-SEQUENCING

Three biological replicates were performed using different batches of developing seeds from WT and *zat5-1*. For each experiment, seeds at 7 to 8 DPA from at least 100 plants were collected and kept in liquid nitrogen. Total RNA was extracted using TRIzol (Invitrogen) according to the manufacturer's instructions and then treated with RNase-free DNase I (Qiagen) to remove genomic DNA. The generation of sequencing libraries and RNA-seq were carried out by Beijing Novogene Bioinformatics Technology (Beijing, China). The libraries were sequenced using the Illumina HiSeq X Ten platform to produce 125 bp/150 bp paired-end raw reads from each library. Cleaned reads from each sample were mapped to the *Arabidopsis* reference genome (Arabidopsis Information

Published in : The Plant Cell (2024), vol. 36, n°10, pp. 4491–4510
DOI: 10.1093/plcell/koae209
Status : Postprint (Author's version)

Resources 10—TAIR10) by HISAT (version 2.2.1). StringTie (version 2.1.4) was then used to assemble transcripts based on the alignment results. Fragments per kilobase of exon per million mapped reads (FPKM) were performed to compute the expression levels of genes. Differential gene expression analysis was conducted by DESeq2 (version 1.18.0). The thresholds for significant differential expression between WT and mutants were set with a *P* value of <0.05 and fold changes of >0.5.

DUAL-LUC ACTIVITY ASSAY

For the effector constructs, the full-length CDS of *ZAT5* was generated by PCR and introduced into the pGreenII 62-SK vector. For the reporter constructs, an ~2-kb DNA sequence upstream from the ATG of PME genes (*PME5*, *HMS*/*PME6*, *PME12*, *PME16*, and *PME58*) was cloned and separately inserted into the pGreenII 0800-LUC reporter. The primers used are listed in Supplementary Table S3. We used pSoup-P19 as the helper plasmid to co-transfect *N. benthamiana* leaves with pGreenII 62-SK-ZAT5 (overexpression) and pGreenII 0800-LUC containing the 5‘ upstream sequences of the *PME* genes. Four co-transfected groups were used. Control co-transfection group 1: pGreenII 0800-LUC and pGreenII 62-SK. Control co-transfection group 2: pGreenII 0800-LUC-promoter and pGreenII 62-SK. Control co-transfection group 3: pGreenII 0800-LUC and pGreenII 62-SK-ZAT5. Co-transfection group 4: pGreenII 0800-LUC- promoter and pGreenII 62-SK-ZAT5. Infected leaves were harvested after 3 d. The firefly LUC and *Renilla* luciferase (REN) activities were then determined using the Dual-Luciferase Reporter Assay Kit (Promega) in accordance with the manufacturer's instructions. Each combination was repeated 5 times. The primers used are shown in Supplementary Table S3.

YEAST ONE-HYBRID ASSAY

A Y1H assay was performed to determine if ZAT5 interacts with DNA sequences within 2-kb upstream from the ATG of the target genes. The full-length CDS of *ZAT5* was transferred into the pGADT7 vector as a prey expression construct. For bait expression vectors, a ~2-kb DNA fragment upstream from the ATG of *PME5*, *HMS*/*PME6*, *PME12*, and *PME16* was amplified and separately fuzed

into the upstream region of the *LacZ* reporter gene in the pLacZi vector. The primers used are shown in Supplementary Table S4. The prey construct and the bait construct were co-transformed into yeast using the One-Hybrid System protocol (TaKaRa, Tokyo, Japan). A pGADT7 empty vector was used as a negative control and a p53-AbAi used as a positive control. The confirmed transformants were grown for 2 to 3 d at 30 °C on SD-Leu/-Ura selective medium.

ELECTROPHORETIC MOBILITY SHIFT ASSAYS

The 858 bp full-length CDS of *ZAT5* was generated and introduced into the pMAL-C2X vector with a MBP tag. The 2,217 bp full-length CDS of *BLH2* was generated and introduced into the pGEX-4T-1 vector with a GST tag. These constructs were separately expressed in *Escherichia coli* BL21 cells, which were then induced at 16 °C with isopropyl β-D-thiogalactoside (1 mM). The fusion proteins

Published in : The Plant Cell (2024), vol. 36, n°10, pp. 4491–4510
DOI: 10.1093/plcell/koae209
Status : Postprint (Author's version)

were purified using glutathione Sepharose 4B (GE Healthcare, 17-0756). Subfragments of candidate gene promoters were amplified and 5′-labeled with biotin by Sangon Biotech Company (Shanghai, China). Each sample included about 1 mg of purified recombinant protein incubated with 50 nM biotin-labeled probes. The EMSA was performed using the LightShift Chemiluminescent EMSA Kit (Thermo Scientific, USA) according to the manufacturer's instructions. The sequences of the DNA probes used are shown in Supplementary Table S5.

CHIP-QPCR ASSAY

Three biological replicates from different batches of siliques were used. For each replicate, we harvested ~2 g siliques at the 7 to 10 DPA stages from WT and *proZAT5:ZAT5:zat5-MYC* T2 generations of transgenic plants and then cross-linked them with aq. formaldehyde (1% *w*/*v*). After terminating cross-linking with glycine (2.5 mL 2 M), the chromatin complexes were extracted and sonicated to give fragments in the range of 200 to 1,000 bp. A portion of the chromatin fragments (~1%) were kept for nonprecipitated total chromatin (input) for normalization. The remaining material was immunoprecipitated with MYC-specific antibodies (Abcam). The purified ChIP products and input DNA samples were quantified by qPCR with the specific primers shown in Supplementary Table S2. The enrichment values were normalized to those of the input sample.

CO-IP ASSAYS

The *Pro35S:MYC-ZAT5*, *Pro35S:BLH2-GFP*, and *Pro35S:BLH4-GFP* vectors were constructed for Co-IP experiments in *N. benthamiana* cells. The plasmids containing BLH2-GFP or BLH4-GFP were transiently co-expressed with MYC-ZAT5 in *N. benthamiana* leaves. The leaves were harvested after infiltration and the total protein then extracted using the immunoprecipitation buffer [1 mM EDTA, 150 mM NaCl, 50 mM Tris-HCl, pH 8.0, 1 mM phenylmethylsulfonyl fluorid (PMSF), 1 mM DTT, 0.5% *v*/*v* Triton X-100, and 1x protease inhibitor cocktail tablets (Thermo Scientific)]. The supernatant was then reacted overnight under mild rotation with anti-GFP (TransGen) coupled to protein A+ G agarose beads (Solarbio). The beads were washed with buffer and the proteins then eluted by boiling for 5 min in SDS loading buffer. MYC-ZAT5 was separated by SDS-PAGE and detected by immunoblot with anti-MYC antibodies (TransGen).

PULL-DOWN ASSAY

The purified fusion proteins MBP-ZAT5 and GST-BLH2 were used in pull-down assays. Purified MBP and GST were used as controls.

The purified MBP tag or MBP-ZAT5 fusion protein were used as bait. Bait proteins were reacted for 2 h at 4 °C with MBP beads (GE Healthcare, USA) in 20 mM Tris-HCl, pH 7.5 containing 100 mM NaCl. The beads were washed 3 times with the buffer and then resuspended in the same buffer. GST or GST-BLH2 prey protein was added to the solution. The mixture was kept for 1 h at 4 °C on a rotator. The mixture was then boiled for 5 min in SDS loading buffer. Immunoblots were performed using an anti-GST antibody (TransGen). Proteins were stained with Coomassie Brilliant Blue.

Published in : The Plant Cell (2024), vol. 36, n°10, pp. 4491–4510
DOI: 10.1093/plcell/koae209
Status : Postprint (Author's version)

PHYLOGENETIC ANALYSIS

Twenty protein sequences of the C1-2i subclass of *Arabidopsis* C2H2-type ZFPs were obtained from The Arabidopsis Information Resource (https://www.arabidopsis.org/). MEGA7 was used to construct a neighbor-joining phylogenetic tree with 1,000 bootstrap replications (Kumar et al. 2016). Numbers on the tree indicate bootstrap support (values <50% are not shown). The scale bar represents the number of amino acid substitutions per site. The alignment file is provided in Supplementary File 1. The phylogenetic tree in Newick format is provided in Supplementary File 2.

STATISTICAL ANALYSIS

GraphPad Prism 7 software was used for statistical analysis. A Student's *t*-test or one-way analysis of variance (ANOVA) with Dunnett's or Tukey's multiple comparison test were used to determine statistically significant differences. Statistical tests and replicate numbers are as shown in the figure legends. Data from statistical analyzes are provided in Supplementary Data Set 2.

Published in : The Plant Cell (2024), vol. 36, n°10, pp. 4491–4510
DOI: 10.1093/plcell/koae209
Status : Postprint (Author's version)

ACCESSION NUMBERS

Sequence data from this study can be found in The Arabidopsis Information Resource (TAIR; https://www.arabidopsis.org) under the following accession numbers: *ZAT5* (AT2G28200), *BLH2* (AT4G36870), *BLH4* (AT2G23760), PME5 (AT5G47500), *HMS*/*PME6* (AT1G23200), *PME12* (AT2G26440), *PME16* (AT2G43050), *PME58* (AT5G49180), and *ACTIN2* (AT3G18780). The raw RNA-seq data from this study have been deposited under the accession number: CRA006508 in the Genome Sequence Archive of the Beijing Institute of Genomics BIG Data Center (http://bigd.big.ac.cn/), Chinese Academy of Sciences.

ACKNOWLEDGMENTS

We thank Malcolm A O'Neill for his help with this manuscript.

AUTHOR CONTRIBUTIONS

Y.K. conceived the project. M.X. and Y.K. designed the research. M.X. carried out the research and wrote the paper. M.X., A.D., D.G., J.S., M.C., Z.L., S.L., A.D., G.Z., Y.X., and M.W. assisted in the experiments. Y.K., A.D., A.R., D.G., and Y.G. revised the manuscript.

SUPPLEMENTARY DATA

The following materials are available in the online version of this article.

Supplementary Figure S1. Expression pattern of *ZAT5* in developing seeds.

Supplementary Figure S2. Histochemical analysis of GUS activity in *ProZAT5:GUS* transgenic *Arabidopsis* tissues.

Supplementary Figure S3. Bioinformatics analysis of *ZAT5*.

Supplementary Figure S4. Subcellular localization of ZAT5 protein in *N. benthamiana* cells.

Supplementary Figure S5. The relative volume of demucilaged seeds from WT, *zat5*, F1 progeny of the cross between *zat5* (female parent) and WT (male parent), and *ProZAT5:ZAT5: zat5-1* seeds after shaking for 2 h in water at 200 rpm and staining with ruthenium red.

Supplementary Figure S6. SEM analysis of WT and *zat5* dry seeds.

Supplementary Figure S7. Mucilage weights and monosaccharide composition of WT and *zat5* mutant seeds.

Supplementary Figure S8. ELISAs of the adherent mucilage from the WT and *zat5-2* using the JIM5, JIM7, and CCRC-M38 antibodies.

Supplementary Figure S9. Expression of *ZAT5* and candidate target genes in the seed obtained from the Arabidopsis eFP browser database.

Supplementary Figure S10. Relative expression of *PME5*, *HMS/ PME6*, *PME12*, and *PME16* in 4 DPA siliques and 7, 10, and 13 DPA seed coat.

Supplementary Figure S11. Identification of *pme5*, *pme6*, *pme12*, and *pme16* mutants.

Published in : The Plant Cell (2024), vol. 36, n°10, pp. 4491–4510
DOI: 10.1093/plcell/koae209
Status : Postprint (Author's version)

Supplementary Figure S12. The relative volume of de- mucilaged seeds from WT, *zat5, pme,* F1 progeny of the cross between *pme* (female parent) and WT (male parent), and *zat5-1 pme* double mutant seeds after shaking for 2 h in water at 200 rpm and staining with ruthenium red.

Supplementary Figure S13. The immunolabeling analysis of JIM5, JIM7, and CCRC-M38 antibodies to *pme5-1*, *pme6*, *pme12-1*, and *pme16* seeds.

Supplementary Figure S14. ELISAs of the adherent mucilage from the WT and *pme* mutants using the JIM5, JIM7, and CCRC-M38 antibodies.

Supplementary Table S1. Primers used for genotype identification.

Supplementary Table S2. Primers used for qPCR and RT-PCR analysis.

Supplementary Table S3. Primers used for construction of expression vectors.

Supplementary Table S4. Primers used for Y1H assays.

Supplementary Table S5. Probes used for EMSA experiments.

Supplementary Data Set 1. The differentially expressed genes in *zat5-1* developing seeds compared with wild type.

Supplementary Data Set 2. Statistical analyses.

Supplementary File 1. Multiple sequence alignment for Supplementary Fig. S3.

Supplementary File 2. Newick format of the phylogenetic tree for Supplementary Fig. S3.

FUNDING

This work was supported by the National Natural Science Foundation of China (32372163, 32270273, 32070330, and 32370278) and the Key Science and Technology Project of the China National Tobacco Corporation [110202001023 (JY-06) and 110202201007 (JY-07)]. The distribution of JIM antibodies used in this work was supported in part by National Science Foundation (NSF) grants (DBI-0421683 and RCN 009281).

CONFLICT OF INTEREST STATEMENT. The authors declare no conflict of interest.

DATA AVAILABILITY

The data underlying this article are available in the article and in its online supplementary material.

Published in : The Plant Cell (2024), vol. 36, n°10, pp. 4491–4510
DOI: 10.1093/plcell/koae209
Status : Postprint (Author's version)

References

Amsbury S, Hunt L, Elhaddad N, Baillie A, Lundgren M, Verhertbruggen Y, Scheller HV, Knox JP, Fleming AJ, Gray JE. Stomatal function requires pectin de-methyl-esterification of the guard cell wall. *Curr Biol*. 2016:26(21):2899-2906. https://doi. org/10.1016/j.cub.2016.08.021

Atmodjo MA, Hao Z, Mohnen D. Evolving views of pectin biosynthesis. *Annu Rev Plant Biol*. 2013:64:747-779. https://doi.org/10.1146/ annurev-arplant-042811-105534

Belmonte MF, Kirkbride RC, Stone SL, Pelletier JM, Bui AQ, Yeung EC, Hashimoto M, Fei J, Harada M, Munoz MD, et al. Comprehensive developmental profiles of gene activity in regions and subregions of the *Arabidopsis* seed. *Proc Natl Acad Sci USA*. 2013:110(5): E435-E444. https://doi.org/10.1073/pnas.1222061110

Bethke G, Grundman RE, Sreekanta S, Truman W, Katagiri F, Glazebrook J. Arabidopsis PECTIN METHYLESTERASEs contribute to immunity against *Pseudomonas syringae*. *Plant Physiol*. 2014:164(2):1093-1107. https://doi.org/10.1104/pp.113.227637

Bradford MM. A rapid and sensitive method for the quantitation of microgram quantities of protein utilizing the principle of proteindye binding. *Anal Biochem*. 1976:72:248-254. https://doi.org/10. 1016/0003-2697(76)90527-3

Caffall KH, Mohnen D. The structure, function, and biosynthesis of plant cell wall pectic polysaccharides. *Garbohydr Res*. 2009:344- (14):1879-1900. https://doi.org/10.1016/j.carres.2009.05.021

Clough SJ, Bent AF. Floral dip: a simplified method for *Agrobacterium*-mediated transformation of *Arabidopsis thaliana*. *Plant J*. 1998:16(6):735-743. https://doi.org/10.1046/j.1365-313x. 1998.00343.x

Dauphin BG, Ranocha P, Dunand C, Burlat V. Cell-wall microdomain remodeling controls crucial developmental processes. *Trends Plant Sci*. 2022:27(10):1033-1048. https://doi.org/10.1016/j.tplants. 2022.05.010

Davletova S, Schlauch K, Coutu J, Mittler R. The zinc-finger protein Zat12 plays a central role in reactive oxygen and abiotic stress signaling in Arabidopsis. *Plant Physiol*. 2005:139(2):847-856. https://doi.org/10.1104/pp.105.068254

Desikan R, A-H-Mackerness S, Hancock JT, Neill SJ. Regulation of the Arabidopsis transcriptome by oxidative stress. *Plant Physiol*. 2001:127(1):159-172. https://doi.org/10.1104/pp.127.1.159

Ding A, Tang X, Yang D, Wang M, Ren A, Xu Z, Hu R, Zhou G, O'Neill M, Kong Y. ERF4 and MYB52 transcription factors play antagonistic roles in regulating homogalacturonan de-methylesterification in Arabidopsis seed coat mucilage. *Plant Gell*. 2021:33(2):381-403. https://doi.org/10.1093/plcell/koaa031

Duan C-J, Basle A, Liberato MV, Gray J, Nepogodiev SA, Field RA, Juge N, Ndeh D. Ascertaining the biochemical function of an essential pectin methylesterase in the gut microbe *Bacteroides thetaiotaomi- cron*. *J Biol Ghem*. 2020:295(52):18625-18637. https://doi.org/10. 1074/jbc.RA120.014974

Ezquer I, Mizzotti C, Nguema-Ona E, Gotte M, Beauzamy L, Viana VE, Dubrulle N, Costa de Oliveira A, Caporali E, Koroney A-S, et al. The developmental regulator SEEDSTICK controls structural and mechanical properties of the Arabidopsis seed coat. *Plant Gell*. 2016:28(10):2478-2492. https://doi.org/10.1105/tpc.16.00454

Published in : The Plant Cell (2024), vol. 36, n°10, pp. 4491–4510
DOI: 10.1093/plcell/koae209
Status : Postprint (Author's version)

Francoz E, Ranocha P, Le Ru A, Martinez Y, Fourquaux I, Jauneau A, Dunand C, Burlat V. Pectin demethylesterification generates platforms that anchor peroxidases to remodel plant cell wall domains. *Dev Gell.* 2019:48(2):261-276.e8. https://doi.org/10.1016/j. devcel.2018.11.016

Harpaz-Saad S, Western TL, Kieber JJ. The FEI2-SOS5 pathway and CELLULOSE SYNTHASE 5 are required for cellulose biosynthesis in the Arabidopsis seed coat and affect pectin mucilage structure. *Plant Signal Behav*. 2012:7(2):285-288. https://doi.org/10.4161/psb. 18819

Hocq L, Pelloux J, Lefebvre V. Connecting homogalacturonan-type pectin remodeling to acid growth. *Trends Plant Sci*. 2017:22(1): 20-29. https://doi.org/10.1016/j.tplants.2016.10.009

Hu R, Li J, Wang X, Zhao X, Yang X, Tang Q, He G, Zhou G, Kong Y. Xylan synthesized by Irregular Xylem 14 (IRX14) maintains the structure of seed coat mucilage in *Arabidopsis*. *J Exp Bot*. 2016:67(5):1243-1257. https://doi.org/10.1093/jxb/erv510

Huang J, DeBowles D, Esfandiari E, Dean G, Carpita NC, Haughn GW. The Arabidopsis transcription factor LUH/MUM1 is required for extrusion of seed coat mucilage. *Plant Physiol*. 2011:156(2): 491-502. https://doi.org/10.1104/pp.111.172023

Jaglo KR, Kleff S, Amundsen KL, Zhang X, Haake V, Zhang JZ, Deits T, Thomashow MF. Components of the Arabidopsis C-repeat/ dehydration-responsive element binding factor cold-response pathway are conserved in *Brassica napus* and other plant species. *Plant Physiol*. 2001:127(3):910-917. https://doi.org/10.1104/pp. 010548

Jiang L, Yang S-L, Xie L-F, Puah CS, Zhang X-Q, Yang W-C, Sundaresan V, Ye D. VANGUARD1 encodes a pectin methylesterase that enhances pollen tube growth in the Arabidopsis style and transmitting tract. *Plant Gell*. 2005:17(2):584-596. https://doi. org/10.1105/tpc.104.027631

Kumar R, Meghwanshi GK, Marcianò D, Ullah SF, Bulone V, Toffolatti SL, Srivastava V. Sequence, structure and functionality of pectin methylesterases and their use in sustainable carbohydrate bioproducts: a review. *Int J Biol Macromol*. 2023:244:125385. https:// doi.org/10.1016/j.ijbiomac.2023.125385

Kumar S, Stecher G, Tamura K. MEGA7: molecular evolutionary genetics analysis version 7.0 for bigger datasets. *Mol Biol Evol.* 2016:33(7):1870-1874. https://doi.org/10.1093/molbev/msw054

Le BH, Cheng C, Bui AQ, Wagmaister JA, Henry KF, Pelletier J, Kwong L, Belmonte M, Kirkbride R, Horvath S, et al. Global analysis of gene activity during *Arabidopsis* seed development and identification of seed-specific transcription factors. *Proc Natl Acad Sci USA*. 2010:107(18):8063-8070. https://doi.org/10.1073/pnas.1003530107

Levesque-Tremblay G, Muller K, Mansfield SD, Haughn GW. HIGHLY METHYL ESTERIFIED SEEDS is a pectin methyl esterase involved in embryo development. *Plant Physiol*. 2015a:167(3):725-737. https://doi.org/10.1104/pp.114.255604

Levesque-Tremblay G, Pelloux J, Braybrook SA, Müller K. Tuning of pectin methylesterification: consequences for cell wall biomechanics and development. *Planta*. 2015b:242(4):791-811. https:// doi.org/10.1007/s00425-015-2358-5

Liu H, Xue S. Interplay between hydrogen sulfide and other signaling molecules in the regulation of guard cell signaling and abiotic/biotic stress response. *Plant Gommun*. 2021:2(3):100179. https://doi. org/10.1016/j.xplc.2021.100179

Livak KJ, Schmittgen TD. Analysis of relative gene expression data using real-time quantitative PCR and the 2(-Delta Delta C(T)) method. *Methods*. 2001:25(4):402-408. https://doi.org/10.1006/ meth.2001.1262

Published in : The Plant Cell (2024), vol. 36, n°10, pp. 4491–4510
DOI: 10.1093/plcell/koae209
Status : Postprint (Author's version)

Macquet A, Ralet M-C, Kronenberger J, Marion-Poll A, North HM. In situ, chemical and macromolecular study of the composition of *Arabidopsis thaliana* seed coat mucilage. *Plant Gell Physiol*. 2007:48(7):984-999. https://doi.org/10.1093/pcp/pcm068

Mohnen D, Atmodjo M, Biswal AK, Hunt K, Mohanty SS, GelineoAlbersheim I, Pattathil S, Hahn MG, Amos R, Hao ZY, et al. Advances in understanding plant cell wall pectin synthesis and structure and impact on the biofuel industry. *Pharm Biol*. 2012:50(5):669. https://doi.org/10.3109/13880209.2012.658722

Moller IE, Pettolino FA, Hart C, Lampugnani ER, Willats WG, Bacic A. Glycan profiling of plant cell wall polymers using microarrays. *J Vis Exp*. 2012:(70):e4238. https://doi.org/10.3791/4238

Palin R, Geitmann A. The role of pectin in plant morphogenesis. *Biosystems*. 2012:109(3):397-402. https://doi.org/10.1016/j.biosystems.2012.04.006

Peaucelle A, Braybrook S, Hofte H. Cell wall mechanics and growth control in plants: the role of pectins revisited. *Front Plant Sci*. 2012:3:121. https://doi.org/10.3389/fpls.2012.00121

Peaucelle A, Louvet R, Johansen JN, Salsac F, Morin H, Fournet F, Belcram K, Gillet F, Hofte H, Laufs P, et al. The transcription factor BELLRINGER modulates phyllotaxis by regulating the expression of a pectin methylesterase in *Arabidopsis*. *Development*. 2011:138- (21):4733-4741. https://doi.org/10.1242/dev.072496

Pelloux J, Rustérucci C, Mellerowicz EJ. New insights into pectin methylesterase structure and function. *Trends Plant Sci*. 2007:12(6):267-277. https://doi.org/10.1016/j.tplants.2007.04.001

Qureshi MK, Sujeeth N, Gechev TS, Hille J. The zinc finger protein ZAT11 modulates paraquat-induced programmed cell death in *Arabidopsis thaliana*. *Acta Physiol Plant*. 2013:35:1863-1871. https://doi.org/10.1007/s11738-013-1224-y

Rautengarten C, Usadel B, Neumetzler L, Hartmann J, Bussis D, Altmann T. A subtilisin-like serine protease essential for mucilage release from Arabidopsis seed coats. *Plant J*. 2008:54(3): 466-480. https://doi.org/10.1111/j.1365-313X.2008.03437.x

Ridley BL, O'Neill MA, Mohnen D. Pectins: structure, biosynthesis, and oligogalacturonide-related signaling. *Phytochemistry*. 2001:57(6): 929-967. https://doi.org/10.1016/S0031-9422(01)00113-3

Röckel N, Wolf S, Kost B, Rausch T, Greiner S. Elaborate spatial patterning of cell-wall PME and PMEI at the pollen tube tip involves PMEI endocytosis, and reflects the distribution of esterified and de-esterified pectins. *Plant J*. 2008:53(1):133-143. https://doi.org/ 10.1111/j.1365-313X.2007.03325.x

Saez-Aguayo S, Ralet M-C, Berger A, Botran L, Ropartz D, Marion-Poll A, North HM. PECTIN METHYLESTERASE INHIBITOR6 promotes *Arabidopsis* mucilage release by limiting methylesterification of homogalacturonan in seed coat epidermal cells. *Plant Cell*. 2013:25(1):308-323. https://doi.org/10.1105/tpc.112.106575

Saffer AM. Expanding roles for pectins in plant development. *J Integr Plant Biol*. 2018:60(10):910-923. https://doi.org/10.1111/jipb.12662

Sakamoto H, Araki T, Meshi T, Iwabuchi M. Expression of a subset of the *Arabidopsis* Cys(2)/His(2)-type zinc-finger protein gene family under water stress. *Gene*. 2000:248(1-2):23-32. https://doi.org/10. 1016/S0378-1119(00)00133-5

Sakamoto H, Maruyama K, Sakuma Y, Meshi T, Iwabuchi M, Shinozaki K, Yamaguchi-Shinozaki K. Arabidopsis Cys2/ His2-type zinc-finger proteins function as transcription repressors under drought, cold, and high-salinity stress conditions. *Plant Physiol*. 2004:136(1):2734-2746. https://doi.org/10.1104/pp. 104.046599

Published in : The Plant Cell (2024), vol. 36, n°10, pp. 4491–4510
DOI: 10.1093/plcell/koae209
Status : Postprint (Author's version)

Senechal F, Wattier C, Rusterucci C, Pelloux J. Homogalacturonan-modifying enzymes: structure, expression, and roles in plants. *J Exp Bot*. 2014:65(18):5125-5160. https://doi. org/10.1093/jxb/eru272

Shi D, Ren A, Tang X, Qi G, Xu Z, Chai G, Hu R, Zhou G, Kong Y. MYB52 negatively regulates pectin demethylesterification in seed coat mucilage. *Plant Physiol*. 2018:176(4):2737-2749. https://doi.org/10. 1104/pp.17.01771

Shi H, Wang X, Ye T, Chen F, Deng J, Yang P, Zhang Y, Chan Z. The cysteine2/histidine2-type transcription factor ZINC FINGER OF ARABIDOPSIS THALIANA6 modulates biotic and abiotic stress responses by activating salicylic acid-related genes and C-REPEAT-BINDING FACTOR genes in Arabidopsis. *Plant Physiol*. 2014:165(3):1367-1379. https://doi.org/10.1104/pp.114.242404

Sola K, Dean GH, Haughn GW. Arabidopsis seed mucilage: a specialised extracellular matrix that demonstrates the structure-function versatility of cell wall polysaccharides. *Annu Plant Rev*. 2019:2(4):1085-1116. https://doi.org/10.1002/9781119312994.

apr0691

Turbant A, Fournet F, Lequart M, Zabijak L, Pageau K, Bouton S, Van Wuytswinkel O. PME58 plays a role in pectin distribution during seed coat mucilage extrusion through homogalacturonan modification. *J Exp Bot*. 2016:67(8):2177-2190. https://doi.org/10.1093/ jxb/erw025

Vogel JT, Zarka DG, Van Buskirk HA, Fowler SG, Thomashow MF. Roles of the CBF2 and ZAT12 transcription factors in configuring the low temperature transcriptome of Arabidopsis. *Plant J*. 2005:41(2):195-211. https://doi.org/10.1111/j.1365-313X.2004.02288.x

Voiniciuc C, Dean GH, Griffiths JS, Kirchsteiger K, Hwang YT, Gillett A, Dow G, Western TL, Estelle M, Haughn GW. Flying saucer1 is a transmembrane RING E3 ubiquitin ligase that regulates the degree of pectin methylesterification in *Arabidopsis* seed mucilage. *Plant Cell*. 2013:25(3):944-959. https://doi.org/10.1105/tpc.112. 107888

Volpi C, Janni M, Lionetti V, Bellincampi D, Favaron F, D'Ovidio R. The ectopic expression of a pectin methyl esterase inhibitor increases pectin methyl esterification and limits fungal diseases in wheat. *Mol Plant Microbe Interact*. 2011:24(9):1012-1019. https://doi.org/ 10.1094/MPMI-01-11-0021

Wang M, Xu Z, Ahmed RI, Wang Y, Hu R, Zhou G, Kong Y. Tubby-like protein 2 regulates homogalacturonan biosynthesis in *Arabidopsis* seed coat mucilage. *Plant Mol Biol*. 2019:99(4-5): 421-436. https://doi.org/10.1007/s11103-019-00827-9

Wang M, Yuan D, Gao W, Li Y, Tan J, Zhang X. A comparative genome analysis of PME and PMEI families reveals the evolution of pectin metabolism in plant cell walls. *PLoS One*. 2013:8(8):e72082. https:// doi.org/10.1371/journal.pone.0072082

Willats WG, Orfila C, Limberg G, Buchholt HC, van Alebeek GJ, Voragen AG, Marcus SE, Christensen TM, Mikkelsen JD, Murray BS, et al. Modulation of the degree and pattern of methyl- esterification of pectic homogalacturonan in plant cell walls. Implications for pectin methyl esterase action, matrix properties, and cell adhesion. *J Biol Chem*. 2001:276(22):19404-19413. https:// doi.org/10.1074/jbc.M011242200

Wolf S, Mouille G, Pelloux J. Homogalacturonan methyl- esterification and plant development. *Mol Plant*. 2009:2(5): 851-860. https://doi.org/10.1093/mp/ssp066

Wolf S, Mravec J, Greiner S, Mouille G, Hofte H. Plant cell wall homeostasis is mediated by brassinosteroid feedback signaling. *Curr Biol*. 2012:22(18):1732-1737. https://doi.org/10.1016/j.cub.2012.07.036

Published in : The Plant Cell (2024), vol. 36, n°10, pp. 4491–4510
DOI: 10.1093/plcell/koae209
Status : Postprint (Author's version)

Wormit A, Usadel B. The multifaceted role of pectin methylesterase inhibitors (PMEIs). *Int J Mol Sci*. 2018:19(10):2878. https://doi.org/ 10.3390/ijms19102878

Wu H-C, Bulgakov VP, Jinn T-L. Pectin methylesterases: cell wall remodeling proteins are required for plant response to heat stress. *Front Plant Sci*. 2018:9:1612. https://doi.org/10.3389/fpls.2018. 01612

Xie M, Sun J, Gong D, Kong Y. The roles of Arabidopsis C1-2i subclass of C2H2-type Zinc-finger transcription factors. *Genes (Basel).* 2019:10(9):653. https://doi.org/10.3390/genes10090653

Xu Y, Hu R, Li S. Regulation of seed coat mucilage production and modification in Arabidopsis. *Plant Sci*. 2023:328:111591. https:// doi.org/10.1016/j.plantsci.2023.111591

Xu Y, Wang YP, Du JG, Pei SQ, Guo SQ, Hao RL, Wang D, Zhou GK, Li SJ, O'Neill M, et al. A DE1 BINDING FACTOR 1-GLABRA2 module regulates rhamnogalacturonan I biosynthesis in Arabidopsis seed coat mucilage. *Plant Cell*. 2022:34(4):1396-1414. https://doi. org/10.1093/plcell/koac011

Xu Y, Wang Y, Wang X, Pei S, Kong Y, Hu R, Zhou G. Transcription factors BLH2 and BLH4 regulate demethylesterification of homo- galacturonan in seed mucilage. *Plant Physiol*. 2020:183(1):96-111. https://doi.org/10.1104/pp.20.00011

Xue C, Guan S-C, Chen J-Q, Wen C-J, Cai J-F, Chen X. Genome wide identification and functional characterization of strawberry pectin methylesterases related to fruit softening. *BMC Plant Biol*. 2020:20(1):13. https://doi.org/10.1186/s12870-019-2225-9

Yin M, Wang Y, Zhang L, Li J, Quan W, Yang L, Wang Q, Chan Z. The Arabidopsis Cys2/His2 zinc finger transcription factor ZAT18 is a positive regulator of plant tolerance to drought stress. *J Exp Bot*. 2017:68(11):2991-3005. https://doi.org/10.1093/jxb/erx157

Yu L, Shi D, Li J, Kong Y, Yu Y, Chai G, Hu R, Wang J, Hahn MG, Zhou G. CELLULOSE SYNTHASE-LIKE A2, a glucomannan synthase, is involved in maintaining adherent mucilage structure in Arabidopsis seed. *Plant Physiol*. 2014:164(4):1842-1856. https:// doi.org/10.1104/pp.114.236596

Zablackis E, Huang J, Muller B, Darvill AG, Albersheim P. Characterization of the cell-wall polysaccharides of *Arabidopsis thaliana* leaves. *Plant Physiol*. 1995:107(4):1129-1138. https://doi. org/10.1104/pp.107.4.1129

Zhao X, Qiao L, Wu A-M. Effective extraction of *Arabidopsis* adherent seed mucilage by ultrasonic treatment. *Sci Rep*. 2017:7(1):40672. https://doi.org/10.1038/srep40672